Schweizerische Eidgenossenschaft
Confédération suisse
Confederazione Svizzera
Confederaziun svizra

Eidgenössisches Departement für
Umwelt, Verkehr, Energie und Kommunikation UVEK

Bundesamt für Energie BFE

SOLAR THERMAL PRODUCTION OF ZINC – FINAL STEPS TOWARD SCALE-UP

Final Report

Autor und Koautoren	A. Meier
Beauftragte Institution	PSI – Labor für Solartechnik
Adresse	5232 Villigen PSI
Telefon, E-mail, Internetadresse	056 310 27 88, anton.meier@psi.ch, http://solar.web.psi.ch
BFE Projekt-/Vertrag-Nummer	101050 / 151210
BFE-Projektleiter	P. Renaud
Dauer des Projekts (von – bis)	1.1.2005 -31.12.2007
Datum	23.5.2008

SUMMARY

A 10 kW receiver-reactor prototype (called *ZIRRUS*) was further improved and tested for the solar thermal decomposition of ZnO, which is the 1st step of the two-step water-splitting thermochemical ZnO/Zn cycle. The rotating cylindrical cavity was made of either sintered ZnO or sintered Al_2O_3 tiles placed on top of a multi-layer Al_2O_3-SiO_2-Y_2O_3-based ceramics for thermal shock resistance, mechanical stability, gas diffusion barrier, and thermal insulation. Pre-heated Ar gas was injected for aerodynamic window protection and for minimizing recombination of product gases in the cavity. Experimentation was carried out at *PSI*'s High-Flux Solar Simulator with the direct heating 10 kW reactor prototype subjected to peak radiative fluxes exceeding 5800 suns. The reactor operated without incident for a total of more than 40 h at maximum temperatures – measured behind the ZnO and Al_2O_3 tiles – ranging from 1807-1907 K. Thermal dissociation of ZnO(s) near 2000 K was demonstrated for experimental runs over 4 h in transient ablation mode with up to nine semi-continuous feed cycles of ZnO particles.

A working Zn/O_2 separation device based on the rapid quenching of the Zn/O_2 mixture is ready to be incorporated at the exit of the solar reactor. Zinc yields of up to 94% were obtained when using total Ar/Zn(g) dilution of 530 and a cooling rate of about 10^5 K/s. The fully integrated solar reactor will be scaled up to the pilot scale of 100 kW. A newly developed reactor model that couples radiation, conduction, and convection heat transfer to the reaction kinetics will allow determining optimal operational conditions for matching the feeding rate to the reaction rate and for maximizing solar-to-chemical energy conversion efficiency.

The 2nd step of the ZnO/Zn cycle has been experimentally demonstrated at *ETH* * using an aerosol-flow reactor for in situ formation and hydrolysis of Zn nanoparticles. The reactor was operated continuously at 1 bar and 573-1263 K, yielding up to 90% chemical conversion for a residence time of about 1 s, and producing nanoparticles with mean crystallite sizes in the 40-100 nm range, containing up to 80 wt% ZnO.

A Life Cycle Assessment (*LCA*)** confirmed that the ZnO/Zn cycle is a promising option for storing solar energy in hydrogen aimed at substituting fossil-based fuels in sustainable future transportation systems.

* Research on $Zn+H_2O$ is being funded by *ETH* Zurich, through the Professorship in Renewable Energy Carriers.
** LCA is being performed within the framework of the Swiss Competence Center Energy and Mobility (*CCEM-CH*).

FOREWORD

This final report contains major contributions from Lothar Schunk (*PSI*) and Aldo Steinfeld (*PSI/ETH*). The solar experimental work was performed at the High-Flux Solar Furnace and at the High-Flux Solar Simulator, Paul Scherrer Institut, Villigen, Switzerland.

ACKNOWLEDGEMENTS

The financial support by the *BFE* Swiss Federal Office of Energy is gratefully acknowledged.

Special thanks go to Urs Wolfer, Bereichsleiter Solarenergie (*BFE*), and Pierre Renaud, Programmleiter Solarchemie (*BFE*), as well as to Alexander Wokaun, Bereichsleiter Allgemeine Energie (*PSI*) for their continuing support of the project.

The invaluable work of the core project team formed by Lothar Schunk, Daniel Gstöhl, Peter Häberling, Samuel Wepf, and Daniel Wuillemin (*PSI*) is gratefully acknowledged.

Many thanks go to Ivo Alxneit and Christian Wieckert (*PSI*) for fruitful discussions.

Special thanks go to Alwin Frei (*PSI*) for chemical analyses, Max Brack and Marco Stricker (*PSI*) for technical support, Anja Weber (*PSI*) for SEM photographs.

The next acknowledgement is to Patrick Coray (*PSI*) and Hansmartin Friess (*ETH*) for assistance in Computational Fluid Dynamics (CFD) and Monte-Carlo ray-tracing (*MC*) simulations.

We welcomed the contributions of many *ETH* students: Kevin Cuche, Laurent Donati, Michael Gasser, Valerio Gianini, Enrico Giulielmini, Remo Hotz, Dominique Kronenberg, Patrick Leu, Frank Lienhard, Stephan Meder, Christoph Meier, Niklas Rotering, Michael Schmid, Clemens Suter, Patrick Vielle, Frederik Wiedmer.

Many thanks go to students from foreign universities: Andrea Brambilla and Davide Colzani (Politecnico di Milano, Italy), Sebastian Möllencamp (University of Applied Science, Groningen, Netherlands).

Diese Arbeit ist im Auftrag des Bundesamtes für Energie entstanden.
Für den Inhalt und die Schlussfolgerungen sind ausschliesslich die
Autoren dieses Berichts verantwortlich.

TABLE OF CONTENTS **Page**

Projektziele – Project Goals

Research on the "Solar Thermal Production of Zinc" is continued at *PSI*'s Solar Technology Laboratory with financial support of *BFE*. We report on the 3-years project *Solar Thermal Production of Zinc – Final Steps Toward Scale-up* (2005-07) [1], which is the follow-up project of *Solar Chemical Reactor Engineering for the Solar Thermal Production of Zinc* (2003-04) [2].

1. MOTIVATION

The principal motivation behind this research is the conviction that solar energy can contribute significantly to the world economy. To help realize this vision, *PSI*'s Solar Technology Laboratory is focused on developing solar thermal chemical reactors that are technically feasible at an industrial scale and operate with a high conversion efficiency of sunlight to chemical energy [3],[4].

Solar-driven water-splitting thermochemical cycles offer the potential of energy efficient large-scale production of hydrogen [4]-[6]. Of special interest is the two-step cycle based on the ZnO/Zn redox reactions, comprising: (1) the endothermic thermal dissociation of ZnO(*s)* into Zn(*g)* and O_2 at above 2000 K using concentrated solar energy as the source of process heat; and (2) the non-solar exothermic hydrolysis of Zn to form H_2 and ZnO(*s)*. This water-splitting cycle has been identified as a promising path for solar hydrogen production because of its potential of reaching high energy conversion efficiencies and consequently economic competitiveness [7]-[9]. Assuming a reactor temperature of 2000 K, an incident solar concentration ratio of 5000, and a 50% sensible and latent heat recovery, the theoretical solar-to-fuel reactor efficiency exceeds 40%.

The second step of the cycle has been experimentally demonstrated at *ETH*[1] using an aerosol-flow reactor for in situ formation and hydrolysis of Zn nanoparticles [10],[11]. For the first solar step, the proposed chemical reactor concept is based on a rotating cavity receiver lined with ZnO particles that are held by centrifugal force and directly exposed to high-flux irradiation [12]. With this arrangement, ZnO serves simultaneously as radiant absorber, chemical reactant, and thermal insulator. ZnO*(s)* is dissociated at high temperatures to its elements in the solar reactor and the Zn*(g)* is separated from the O_2 through a rapid quench of the products. The Zn*(s)* is then used either directly in a Zn/air fuel cell or battery for electricity generation or it is used to produce hydrogen, when and where it is needed. In either scenario, the chemical by-product is ZnO*(s)*, which is eventually recycled to the solar reactor. Sunlight is converted to a storable and transportable fuel in a closed material cycle.

2. PURPOSE

The main purpose of the current research is to complete the chemical and mechanical engineering science and technology base required to scale up a direct heating solar reactor for producing Zn with sunlight in two different high temperature thermo-chemical processes: (1) from pure ZnO*(s)* at temperatures above 2000 K; (2) from ZnO(*s*)/carbon mixtures in a carbothermic process at temperatures near 1400-1800 K. With respect to the chemical reactor technology for the purely solar decomposition of ZnO*(s)*, an important process specific objective is to implement a suitable quench unit based on *PSI*'s latest understanding of the reaction kinetics of the Zn/O_2 recombination reaction [13],[14]. Solving major engineering science and technology problems further involves learning how to keep the reactor window clean in the course of a day and testing the rotating reactor as it will be used in an industrial solar process on top of a solar tower.

Goals for the current project concerned two main topics: (A) modification and optimization of 10 kW solar reactor prototype; (B) process demonstration at laboratory scale including validation of numerical reactor model.

(A) **Reactor specific goals** encompass

(1) Selection and testing of appropriate *high-temperature cavity wall materials* capable of withstanding the high temperature, thermal shock, and severe chemical conditions for the two solar chemical reactions under consideration. While the carbothermic ZnO*(s)* decomposition proceeds at temperatures around 1400-1800 K without any material problems, further material test cycles are essential for the thermal dissociation of ZnO*(s)* in the temperature range 1800-2200 K.

---

[1] Research on $Zn+H_2O$ is being funded by *ETH* Zurich, through internal funds of the Professorship in Renewable Energy Carriers.

(2) Investigation of *high-temperature ceramic insulation materials* used as thermal insulation of front and aperture region, cavity, feeder tip, etc. In particular, chemical stability against reactions with ZnO requires further testing.

(3) Q*uenching* of the ZnO*(s)* dissociation products at the exit of the solar reactor. Essential is the fundamental understanding of the $Zn_{(g)}/O_2$ recombination reaction for the non-carbothermic ZnO*(s)* decomposition process [13].

(4) Development of a reliable method for keeping the reactor window clear of condensed reaction products. Of particular interest is an *aerodynamic window protection* system requiring Computational Fluid Dynamics (*CFD*) simulations.

Optional goals with regard to future scale-up:

(5) Utilization of a secondary concentrator (*CPC*) mounted in front of the reactor's aperture to ensure sufficient solar concentration for reaching the required temperatures.

(6) Adaption of the solar *reactor orientation* since it is anticipated that an industrial reactor will operate at some angle from the horizontal, close to about 45 degrees downward if it is used in a tower.

(7) Thermal efficiency of the 10 kW solar reactor prototype exceeding 10%.

(B) **Process specific goals** include

(8) Demonstration of *quasi-continuous reactor operation* during more than 4 hours without mechanical or process problems. Reliable reactor operation for more than 50 hours.

(9) Completion of the *performance map* of the 10 kW solar reactor prototype (measuring radiative flux, temperature, and gas composition; closing gas and mass balance) and comparison to the numerical transient heat transfer model describing many of the physical processes taking place in the reactor.

Optional goals with regard to process optimization:

(10) Demonstration of the "ablation" mode of operation by conducting experimental runs of short periods of time under transient condition.

(11) ZnO dissociation rate in 10 kW solar reactor exceeding 0.5 kg/hr.

3. STATE-OF-THE-ART IN CONTEXT WITH SOLAR CHEMISTRY RESEARCH AT PSI

A comprehensive review of the science and technology for solar thermochemical processes can be found in [3],[4]. Here, we present the state-of-the-art in context with solar chemistry research at *PSI*.

3.1. Concentration of Solar Energy

Concentrating solar power (CSP) – The state-of-the-art technology for the large-scale collection and concentration of solar energy relevant for solar chemical processes involving solid-gas reactions is based on solar tower systems as shown schematically in Fig. 1. Such tower systems use a field of heliostats (two-axis tracking parabolic mirrors) that focus the sunrays onto a solar receiver mounted on top of a centrally located tower. A recently developed Cassegrain optical configuration for the tower system makes use of a hyperboloidal reflector at the top of the tower to re-direct sunlight to a receiver located on the ground level (Fig. 2) [15]. These solar concentrating systems have been proven to be technically feasible in large-scale experimental demonstrations aimed mainly at the production of solar thermal electricity in which a working fluid (typically air, water, helium, sodium, or molten salt) is solar-heated and further used in traditional Rankine or Brayton cycles. The first commercial concentrating solar power (*CSP*) tower plant is in operation since March 2007 near Seville, Spain. The 11 MW_e thermoelectrical plant with saturated steam receiver (*PS10* [16],[17]) is shown in Fig. 1. A similar 20 MW_e solar thermal power plant (PS20) is currently under construction. Solar thermochemical applications, although not developed as far as solar thermal electricity generation, employ the same solar concentrating technology.

The solar flux concentration ratio typically obtained at the focal plane varies between 500-1,000 suns (1 sun = 1 kW/m^2) for solar tower systems. To some extent, the flux concentration can be further augmented with the help of non-imaging secondary concentrators, e.g., a compound parabolic concentrator, referred to as *CPC* [18], which are positioned in tandem with the primary concentrating systems. Higher concentration ratios imply lower heat losses from smaller receivers and, consequently, higher attainable temperatures at the receiver.

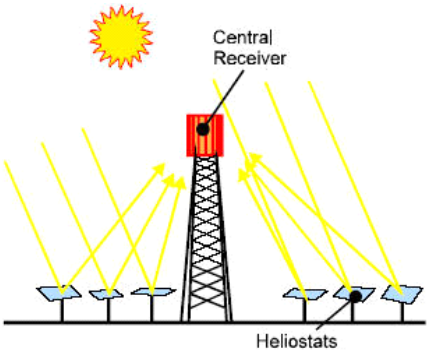

Figure 1: Left: schematic of the concentrating solar power (*CSP*) tower or "tower top" system. Right: aerial view of the 11 MW_e thermoelectric plant *PS10* in operation (foreground) and the 20 MW_e plant *PS20* under construction (background) near Seville, Spain [16],[17]. www.solucar.es

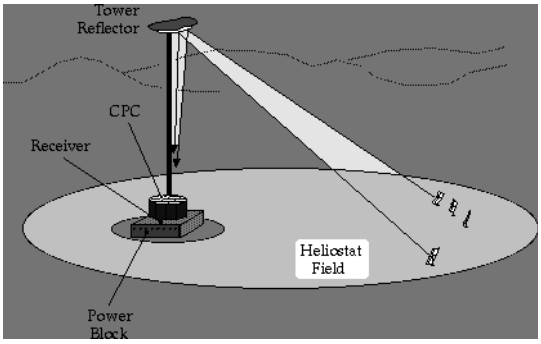

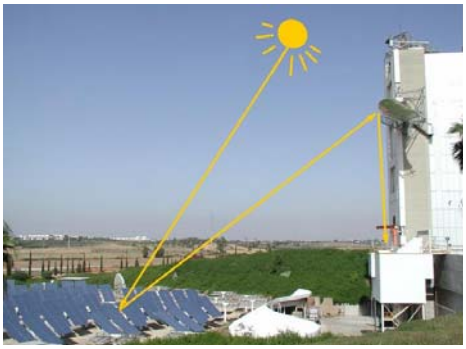

Figure 2: Left: schematic of the solar tower reflector or "beam down" system [15]. Right: Solar Research Facility at Weizmann Institute of Science, Rehovot, Israel.

PSI's concentrating solar research facilities – *PSI*'s two state-of-the-art major experimental facilities, namely the High-Flux Solar Furnace (*HFSF*) [19], Fig. 3, and the High-Flux Solar Simulator (*HFSS*) [20], Fig. 4, serve as unique experimental platforms for investigating the thermochemical processing of solar fuels, for testing advanced ceramic materials at temperatures up to 3,000 K and heating rates up to 1,000 K/s, and for validating radiation heat transfer models applied in the development of high-temperature thermochemical reactors.

Figure 3: *PSI*'s High-Flux Solar Furnace (*HFSF*) consists of a 120 m² sun-tracking flat heliostat on-axis with an 8.5 m diameter paraboloidal concentrator [19]. It delivers up to 40 kW at peak concentration ratios exceeding 5000 suns (1 sun = 1 kW/m²). The solar flux intensity can be further augmented to up to 10,000 suns by using *CPC* secondary concentrators. A Venetian blind type shutter located between the heliostat and the concentrator controls the power input to the reactor. http://solar.web.psi.ch/

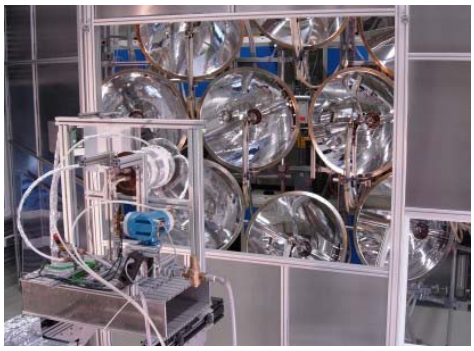

Figure 4: *PSI*'s High-Flux Solar Simulator (*HFSS*) comprises an array of ten 15 kW_e high-pressure Xenon arcs, each close-coupled with truncated ellipsoidal specular reflectors of common focus [20]. This facility is able to deliver a total radiative power of 50 kW with a peak radiative flux exceeding 10,000 suns. The total radiative power intercepted by a 6 cm diameter circular target – representing the reactor's aperture – is 20 kW, and the average radiative power flux over this aperture is more than 7,000 suns.

3.2. Storage of Solar Energy

Thermal energy storage

Most *CSP* plants under development are equipped with a thermal storage system [21]. Currently, thermal energy storage (*TES*) is the most innovative and therefore the most risky component of a *CSP* system. Application of thermal storage optimizes the economy of a *CSP* system by more levelized production and better controllability. The best suitable type of storage system depends on the heat transfer fluid (*HTF*), the pressure and the capacity used in the *CSP* plant. For the short term, thermal storage in molten salts dominates the commercial developments in Spain (*Andasol*: two 50 MW_e parabolic trough plants under construction; *Solar Tres*: 15 MW_e solar tower concept) and was previously tested in the USA (*Solar Two*: 10 MW_e solar tower test facility). Cost reductions up to 30% are estimated [22]. For the longer term, thermal storage in cement and ceramics is thought to be a factor two more cost effective. This type of storage is under development [23]. Thermal energy storage systems are designed to shift energy for some hours (e.g. from day time to evening).

Chemical energy storage

The limitations of thermal energy storage in time (hours) and space (on-site) can be overcome by converting concentrated solar energy into chemical energy carriers – *solar fuels* – that can be stored long time and transported long range.

Thermochemical production of hydrogen – Hydrogen is envisioned as an important energy vector of the future. Five thermochemical routes for solar hydrogen production are depicted in Fig. 5. Indicated is the chemical source of hydrogen (H_2): water (H_2O) for the solar thermolysis and the solar thermochemical cycles; fossil fuels for the solar cracking, and a combination of fossil fuels and H_2O (steam) for the solar reforming and solar gasification. All of these routes involve endothermic reactions that make use of concentrated solar radiation as the energy source of high-temperature process heat.

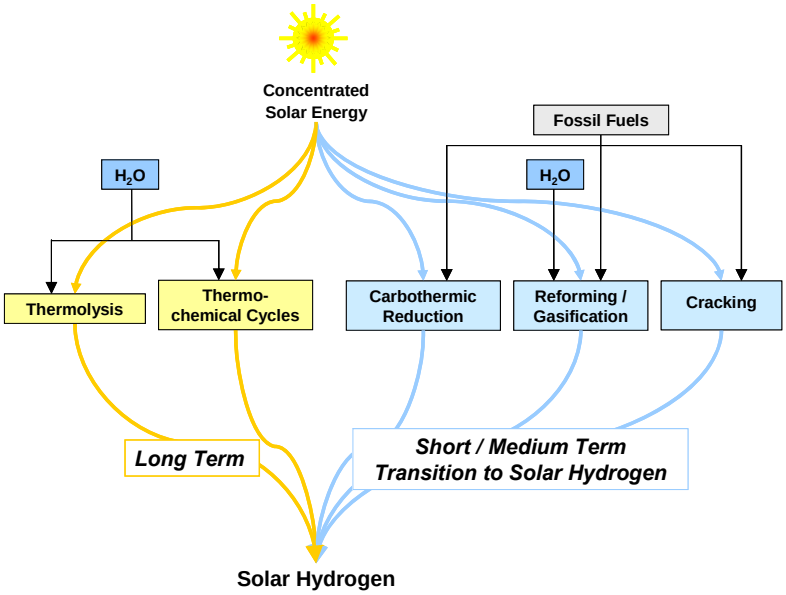

Figure 5: Five thermochemical routes for the production of solar hydrogen.

H_2 by decarbonization of fossil fuels – The short/mid-term transition to solar hydrogen is favored by thermochemical processes that upgrade the calorific value of fossil fuels such as natural gas, oil, and coal using process heat from concentrated solar energy. Such hybrid processes for hydrogen production include cracking and reforming/gasification. The solar cracking refers to the thermal decomposition of hydrocarbons to co-produce primarily hydrogen and solid carbon black that can either be sequestered without CO_2 release or used as a material commodity or metallurgical reducing agent under less severe CO_2 restraints [24]-[28]. The steam reforming of hydrocarbons [29]-[31], and the steam gasification of coal and other solid carbonaceous materials [32]-[34] yield synthesis gas (*syngas*), which can be further processed to hydrogen via the catalytic water-gas shift reaction followed by the separation of hydrogen and carbon dioxide.

Zn from carbothermic reduction of ZnO – The carbothermic reduction of metal oxides for the production of metals and the subsequent hydrolysis to produce hydrogen also belongs to this category of hybrid solar/fossil fuel processes. An example is the solar carbothermic reduction of ZnO(*s*) for the production of Zn that was investigated in the Solar Technology Laboratory's *EU* project, *SOLZINC* [35],[36].

H_2 from H_2O by solar thermolysis – One of the long-term goals of solar chemistry is the pure solar production of hydrogen. The single-step thermal dissociation of water, known as water thermolysis, although conceptually simple, has been impeded by the need of a high-temperature heat source at above 2500 K for achieving a reasonable degree of dissociation, and by the need of an effective technique for separating H_2 and O_2 to avoid recombination or ending up with an explosive mixture. Among the ideas proposed for separating H_2 from the products are effusion and electrolytic separation [37]-[40].

H_2 from H_2O by solar thermochemical cycles – Water-splitting thermochemical cycles bypass the H_2/O_2 separation problem and further allow operating at relatively moderate upper temperatures. Previous studies performed on water-splitting thermochemical cycles were mostly characterized by the use of process heat at temperatures below about 1300 K, available from nuclear and other thermal sources. These cycles require multiple steps (more than two) and suffer from inherent inefficiencies associated with heat transfer and product separation at each step. In recent years, significant progress has been made in the development of optical systems for large-scale collection and concentration of solar energy capable of achieving solar concentration ratios of 5,000 suns and higher. Such high radiation fluxes allow the conversion of solar energy to thermal reservoirs at 2000 K and above, which are needed for the more efficient two-step thermochemical cycles using metal oxide redox reactions [41], and literature cited therein.

Chemical energy storage based on ZnO/Zn cycle

Chemical energy storage based on the solar thermochemical ZnO/Zn cycle offers flexible storage of solar energy both in time and space. In a project endorsed by the International Partnership for the Hydrogen Economy (*IPHE*) [42], the ZnO/Zn cycle has been identified as one of the most promising candidates for the solar driven high temperature thermochemical production of hydrogen. Within the *EU* project *INNOHYP-CA* it has also been selected as one of the 12 most innovative high temperature processes for hydrogen production [43]. Comprehensive literature reviews on solar thermochemical processing have been carried out by [3]-[5],[44].

Figure 6 shows a schematic representation of the ZnO/Zn thermochemical storage cycle. In this process, concentrated sunlight provides high-temperature process heat for the endothermic reaction:

$$ZnO \rightarrow Zn + ½\ O_2 \qquad (1)$$

At temperatures near 2000 K, the reaction proceeds. Solar radiation is thereby directly converted into the chemical energy of Zn and O_2. To avoid their recombination at high temperature, the gas phase products Zn(g) and O_2 are separated with a rapid cooling process known as a quench. The solar energy stored in the condensed Zn phase may be used as the fuel in an advanced Zn-air electricity generator (combination of fuel cell and battery) to generate electricity:

$$Zn + ½\ O_2 \rightarrow ZnO \qquad (2)$$

When hydrogen is the desired fuel, it has also been suggested that the Zn be used to split water in an exothermic reaction:

$$Zn + H_2O \rightarrow ZnO + H_2 \qquad (3)$$

Hydrogen may be converted to electricity in a H_2-O_2 fuel cell, predominantly for mobile applications:

$$H_2 + ½\ O_2 \rightarrow H_2O \qquad (4)$$

In either scenario, the ZnO is recycled to the solar process (2´, 3´), thus closing the cycle.

Zn from thermal dissociation of ZnO – Several chemical aspects of the thermal dissociation of ZnO have been investigated [7],[45]. At 2340 K, $\Delta G° = 0$ and $\Delta H° = 395$ kJ/mol. The exergy efficiency of the solar thermochemical two-step water-splitting ZnO/Zn cycle (reactions 1 and 3) is estimated at 35% without heat recovery of the quench or hydrolysis process. The theoretical upper limit on efficiency with total heat recovery is 82% when operating the solar reactor at 2000 K. As an alternative to the quench, electro-thermal methods for *in-situ* separation of Zn(g) and O_2 at high temperatures have been experimentally demonstrated to work in small scale reactors [40]. High-temperature separation further enables recovery of the sensible and latent heat of the products (e.g., 116 kJ/mol during Zn

condensation). Various exploratory tests on the dissociation of ZnO were carried out in solar furnaces [46]-[48]. A solar chemical reactor concept was designed [12] and modified [49]. Solar tests carried out with a 10 kW reactor prototype subjected to a peak solar concentration of 4000 suns proved the low thermal inertia of the reactor system – ZnO surface temperature reached 2000 K in 2 seconds – and its resistance to thermal shocks.

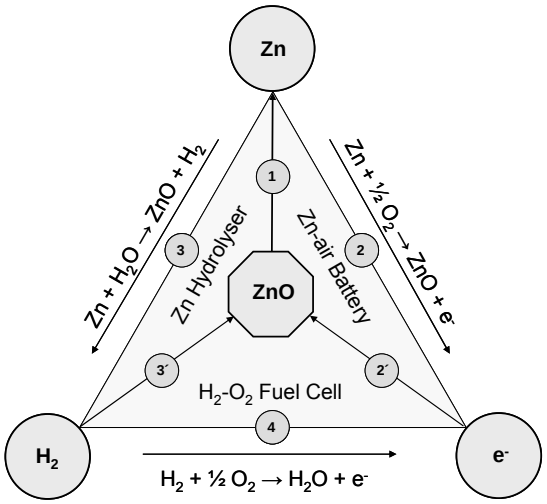

Figure 6: Schematic representation of the ZnO/Zn thermochemical storage cycle: Zn is produced by endothermic solar thermal dissociation of ZnO using concentrated solar energy as the source of process heat at 2000 K: ZnO → Zn + ½ O_2 (1). Electricity is generated either directly from Zn in a Zn-air electricity generator (2) or via production of H_2 by Zn hydrolysis (3) followed by conversion in a H_2-O_2 fuel cell (4). In either case, ZnO is recycled to the solar process (2´, 3´), thus closing the cycle. Both Zn and H_2 are solar fuels storing solar energy in the form of chemical energy. (Source: *PSI*)

Zn-air electricity generation – Today, no commercially available equipment exists for bulk electricity generation based on metal-air fuel cell or battery technology envisioned for future applications. However, the metal-air battery technology currently being developed can be used as a starting point for the large-scale metal-air electricity generation technology making use of a metal that is oxidized with oxygen from the air while generating electricity. Among the different metal-air batteries, Zn-air batteries are at the most advanced stage of development[2]. This coincides favorably with the fact that ZnO has one of the lowest thermal decomposition temperatures of metal oxides (which determines the operating temperature of the solar reactor), thus providing excellent opportunities for the ZnO/Zn-based solar energy storage technology.

H_2 from Zn hydrolysis – An alternative pathway for electricity generation is based on the on-demand production of hydrogen from solar produced zinc and the subsequent use of the hydrogen, e.g. in a fuel cell powering a car. Here, the production of H_2 is realized via the hydrolysis of Zn, as described in reaction (3) and illustrated in Fig. 6. The ZnO originating from this reaction will serve as the feedstock for the solar ZnO dissociation reactor. In principle, the heat liberated by the exothermic reaction (3), 104 kJ/mol, could be used in an auto-thermal type of hydrolyser to produce steam and to melt or vaporize Zn (Zn melting point 419°C, boiling point 907°C).

Investigations of a novel process encompassing the formation of Zn nano-particles followed by their in-situ steam hydrolysis for H_2 production have been initiated at *ETH*[3] [9]. This combined process was experimentally demonstrated using a tubular hot-wall aerosol flow reactor with separated evaporation, cooling and reaction zones shown in Fig. 7 [11]. Superheated Zn vapor was carried by Ar into a tubular quartz reactor, where it was mixed and quenched by a superheated, equimolar H_2O/Ar stream resulting in the formation of Zn/ZnO nanoparticles and H_2. The Zn(g) vapor was generated by electric heating of a Zn crucible whose weight was continuously monitored and compared to the H_2 production rate. The reactor was operated continuously at 1 bar and 573-1263 K, yielding up to 90% chemical conversion (Fig. 7) for a residence time of about 1 s, and producing nanoparticles with mean crystallite sizes in the 40-100 nm range, containing up to 80 wt% ZnO.

---

[2] Contacts are established to the company ReVolt located in Switzerland, which is a key player in the area of Zn-air batteries. ReVolt Technology Limited, 8712 Stäfa Switzerland, www.revolttechnology.com

[3] Research on Zn+H_2O is being funded by *ETH* Zurich, through internal funds of the Professorship in Renewable Energy Carriers.

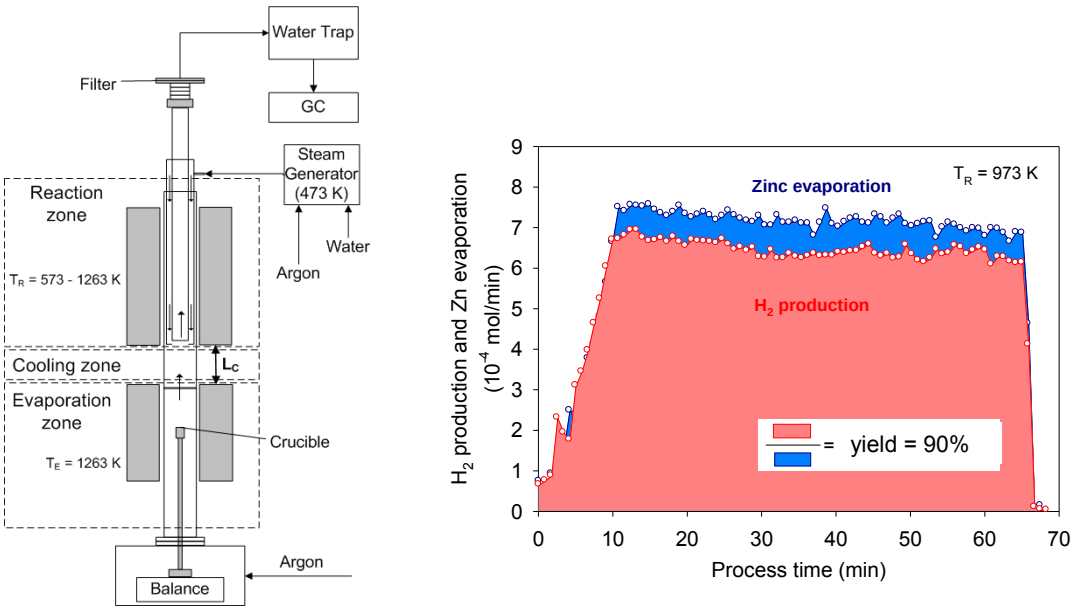

Figure 7: Left: Apparatus for co-synthesis of H_2 and Zn/ZnO particles by *in-situ* formation and hydrolysis of Zn aerosol, featuring distinct evaporation, cooling, and chemical reaction zones where the high temperature particle residence time can be controlled separately. Right: Molar rates of Zn evaporation and H_2 production at 973 K, yielding up to 90% chemical conversion. From [11].

3.3. Life Cycle Assessment (LCA) of Solar Hydrogen Production [4]

In the framework of a Ph.D. Thesis [50], a well-to-wheel analysis has been conducted for future production, transport, and usage of solar hydrogen in passenger cars [51]. The life cycle assessment (*LCA*) included a quantification of greenhouse gas (*GHG*) emissions, the cumulative energy demand (*CED*) and two life cycle impact assessment (*LCIA*) methodologies. Figure 8 shows scenarios for solar hydrogen being produced in a concentrating solar power (*CSP*) plant located in Southern Spain and transported to Central Europe exemplified by Switzerland. The two-step ZnO/Zn water-splitting cycle, either based on the solar thermal dissociation (*STD*) of ZnO at above 2000 K or, alternatively, on the solar carbothermic reduction (*SCR*) of ZnO at about 1500 K, has been identified as a promising path for solar hydrogen production because of its potential of reaching high energy conversion efficiencies, and consequently, the potential of economic competitiveness [9]. The benchmark is solar hydrogen production by water electrolysis using solar thermal electricity (*STE*) generated in a *CSP* plant. The solar hydrogen production methods have been compared with selected conventional production technologies, such as steam methane reforming (*SMR*) and coal gasification (*CGA*), as well as with alternative pathways such as water electrolysis using locally produced hydro or nuclear power.

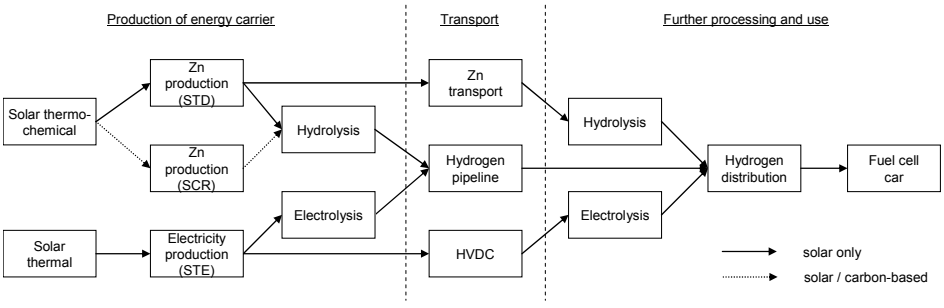

Figure 8: Pathways for (1) solar production of H_2 at *CSP* plant located in Southern Spain; (2) transport to Central Europe (Switzerland) of either H_2 in pipelines ("*pipe*"), or Zn by freight ship and rail ("*zinc*"), or electricity by high voltage direct current transmission lines ("*hvdc*"); (3) distribution and utilization of H_2 in fuel cell vehicle (*FCV*). From [51].

[4] *LCA* was performed within the framework of the Swiss Competence Center Energy and Mobility (*CCEM-CH*), Project "Transition to hydrogen based transportation"; Ph.D. Thesis was funded by the *Baugarten Foundation*.

Solar scenarios (*STD, STE*) reduce greenhouse gas (*GHG*) emissions for the production of hydrogen compared to conventional technologies by a factor of 7 (*SMR*) and 14 (*CGA*), which eventually results in 50-70% CO_2 savings in a *FCV* (Fig. 9). However, compared to electrolysis using locally produced hydro or nuclear power, *GHG* emissions from *CSP* pathways are distinctly higher due to the steel-intensive infrastructure for the heliostat field and energy transport losses from Southern Spain to Switzerland. Solar thermal dissociation of ZnO with subsequent hydrogen pipeline transport (*STD* pipe) shows the lowest *GHG* emissions of the assessed *CSP* hydrogen technologies. Transporting zinc (*STD* zinc) instead of hydrogen about doubles *GHG* emissions of the fuel chain because of associated transport emissions. Transporting electricity (*STE* hvdc) causes N_2O emissions in the corona of the high voltage transmission lines, which is an extremely strong *GHG* (about 300 times as strong as CO_2).

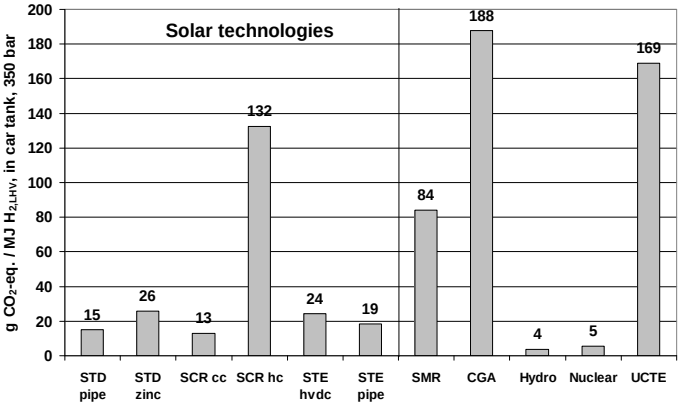

Figure 9: *GHG* emissions in g CO_2-eq. per MJ hydrogen (*LHV*) in car tank at 350 bar. Acronyms defined in text. *UCTE* = European electricity mix 2025. From [51].

Figure 10 depicts passenger car transportation costs for selected scenarios showing contributions of road infrastructure, operation and maintenance (O&M), fuel production and supply, and external costs [52]. Main cost component is O&M, comprising total annual costs for the consumer (consisting to a large extent of car depreciation) excluding fuel costs. High capital investments for heliostat field infrastructure and long-distance transport result in 2.5-5.5 times higher hydrogen production and supply costs for solar scenarios vis-à-vis conventional *SMR* (4 US$/kg H_2 in car tank), depending on the chosen scenario. *STD* with hydrogen pipeline transport (*STD* pipe) costs about 0.07 US$/pkm, corresponding to 14.7 US$/kg H_2 in car tank and 10.1 US$/kg H_2 at plant. *STE* with hydrogen pipeline transport (*STE* pipe) costs about 0.11 US$/pkm (21.9 US$/kg H_2 in car tank and 16.1 US$/kg H_2 at plant). For comparison, the most economic *CSP* options using zinc transport (*STD* zinc) cost around 0.05 US$/pkm or 10.2 US$/kg H_2 in car tank, less than hydrogen fuel costs using hydro or wind electricity for electrolysis (about 0.06 US$/pkm). Total transportation costs may increase by 0.20-0.25 US$/km for a *FCV* powered by solar hydrogen compared to an *ICE* vehicle using gasoline. Assuming long-term market acceptance associated with return on investment being reduced from 15% for new technologies to 5% for established technologies, costs of the most economic *CSP* technology (*STD* zinc) would decrease to 6 US$/kg H_2 and become competitive to costs of *SMR* and *CGA*, which are expected to rise due to fossil resource shortage.

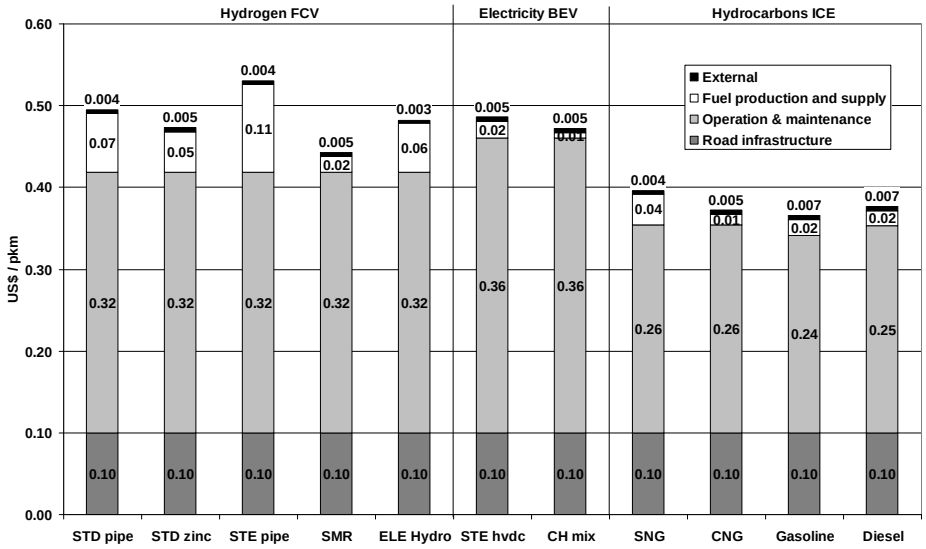

Figure 10: Transportation costs per passenger kilometer (pkm) for selected scenarios with contribution of road infrastructure; O&M (total annual costs for consumer, excluding fuel costs); fuel production and supply; external costs. Average load of 1.59 passengers per car. Details in ref. [50]. From [52].

Durchgeführte Arbeiten und erreichte Ergebnisse – Results

A 10 kW solar reactor prototype (called *ZIRRUS*) was fabricated and tested at *PSI*'s High-Flux Solar Furnace (*HFSF*) by first effecting the carbothermal reduction of ZnO in the range 1400-1800 K [49]. However, at the higher temperatures required for the ZnO dissociation (> 2000 K), mechanical stability problems were encountered with the Hf/HfO_2-based cavity as a result of the heating and cooling cycles and operation in an oxidizing atmosphere [53].

Therefore, an improved reactor was designed that eliminates the material related problems. All reactor components worked well during more than 40 hours of high-temperature testing. The material of construction of the cavity fulfilled the severe requirements of the reaction. The window aerodynamic protection performed well; Zn condensation observed on the quartz window did not prevent continuation of the runs. The reactor was operated in a transient ablation mode with semi-continuous feed cycles of ZnO particles, characterized by a rate of heat transfer – predominantly by radiation – to the layer of ZnO particles undergoing endothermic dissociation that proceeded faster than the rate of heat transfer – predominantly by conduction – through the cavity walls.

The solar reactor technology for the thermal dissociation of ZnO is presented in Chapter 1. Also included is a brief description of the solar thermogravimeter (*Solar TG*) used for high-temperature materials testing and preliminary investigations of new components such as the quench apparatus developed in a parallel *BFE* project [13],[14]. In Chapter 2, the experimental setup and experimental results of the ZnO dissociation are described based on recent publications [54],[55]. Further experimental results concern quench studies [56] and materials tests using the *Solar TG*. Progress in solar reactor and process modeling is summarized in Chapter 3.

1. SOLAR REACTOR TECHNOLOGY

We present the solar reactor technology of the direct heating solar reactor for the ZnO dissociation and the versatile solar thermogravimeter (*Solar TG*) coupled to a novel quench apparatus.

1.1. Direct Heating Solar Reactor

The solar reactor technology for the ZnO dissociation is described in detail in a recent publication [54]. A schematic of the 10 kW solar receiver-reactor prototype for the thermal dissociation of ZnO is depicted in Fig. 11, and a picture of the modular reactor is shown in Fig. 12. Its main component is a 160 mm diameter rotating cylindrical cavity composed of ceramic plates (either sintered ZnO or Al_2O_3 tiles) on top of a porous 80%Al_2O_3-20%SiO_2 insulation reinforced by a 95%Al_2O_3-5%Y_2O_3 ceramic matrix composite (*CMC*) for thermal shock resistance, mechanical stability, gas diffusion barrier, and thermal insulation. Concentrated solar radiation enters the cavity through a 3 mm thick quartz window, which is mounted on a water-cooled aluminum ring and integrated to the front face of the cavity via a conical frustum that contains a 60 mm diameter circular opening – the *aperture*. The reactor has a dynamic feeder that extends and contracts within the cavity, and enables to evenly spread out a layer of ZnO particles of desired thickness along the entire cavity. The rotational movement along the horizontal axis generates a centripetal acceleration that forces the ZnO particles to cover the cavity wall, thereby creating an efficient use of the cavity space for radiation heat transfer to the reaction site. The feeder tip is protected from the hot cavity by a cap made of dense Al_2O_3, compound to a disk of alumina insulation, all packed into a 1 mm thick layer of alumina *CMC*. The feeder can be retracted and scraped clean from deposited solids. Inert gas (Ar) is optionally pre-heated and injected through twelve nozzles located at the window plane, creating an aerodynamic curtain (optimized by *CFD*) that protects the window from condensable Zn(g). Gaseous products Zn(g) and O_2 exit the cavity through a water-cooled annular gap, referred to as the "*quench unit*". The cold walls and the injection of cold Ar promote the rapid quench of Zn(g) to Zn(s).

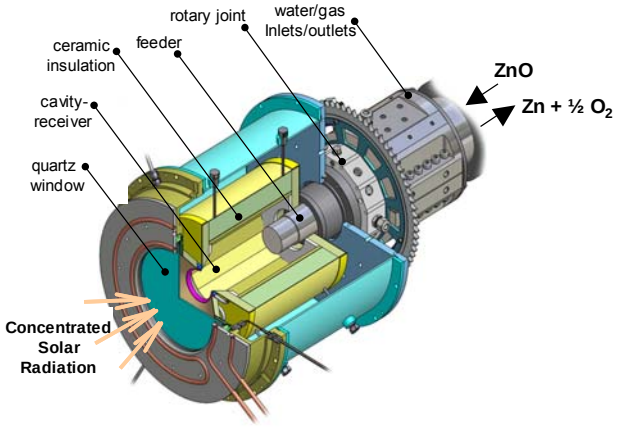

Figure 11: Schematic of the solar chemical reactor configuration. From [55].

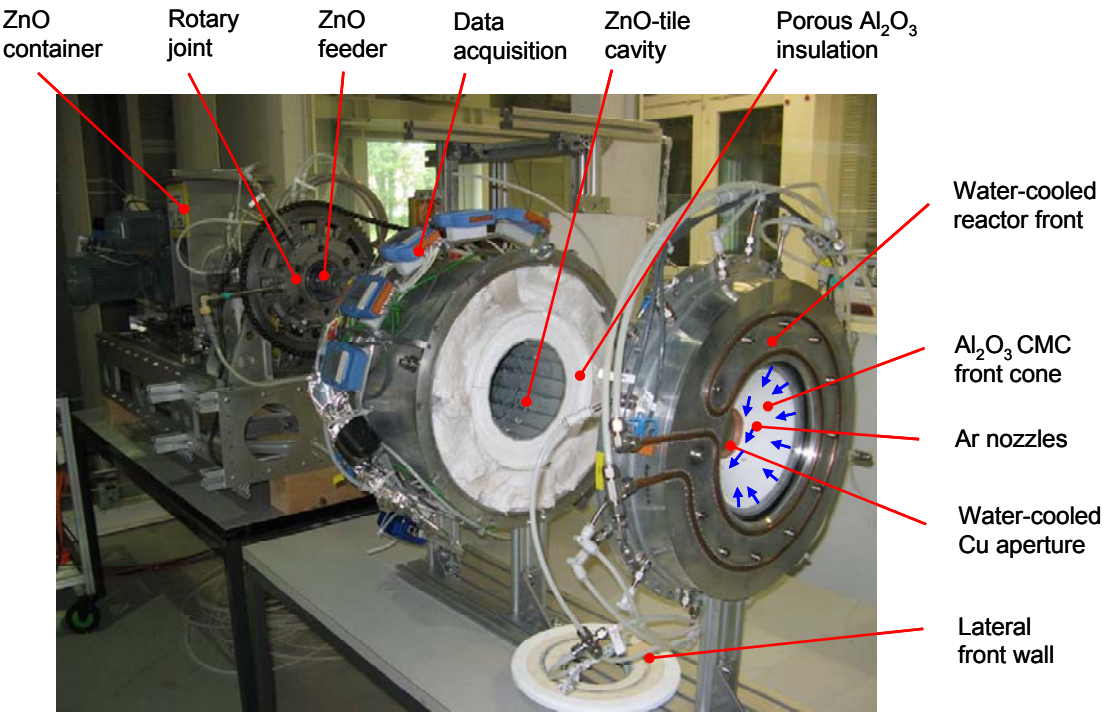

Figure 12: Modular solar reactor components showing from right: Water-cooled reactor front with quartz window and inert gas inlets; insulated rotary cavity with data acquisition system; feeder and rotary joint.

Reactor cavity materials – The innermost cavity layer is made either of 3.7 mm thick sintered ZnO tiles (version 1) or 7 mm thick sintered Al_2O_3 tiles (version 2). Figure 13 shows the arrangement of the 32 sintered ZnO tiles and the porous 80%Al_2O_3-20%SiO_2 insulation on the cavity walls. The ZnO tiles are resistant to thermal shocks, partly due to their relatively high thermal conductivity: 37 $Wm^{-1}K^{-1}$ at room temperature and decreasing to 4 $Wm^{-1}K^{-1}$ at 1273 K [57]. They serve primarily as thermal shock absorber and, to a lower extent, as thermal insulator. The maximum allowable temperature at the interface between tiles and insulation is the eutectic phase temperature of the system ZnO-Al_2O_3-SiO_2 [58], around 1930 K, as determined in separate tests using a thermogravimeter with samples directly exposed to concentrated solar radiation (see below). The outermost cavity layer is made of 1.5 mm thick 95%Al_2O_3-5%Y_2O_3 ceramic matrix composite (*CMC*), which provides both mechanical stability and a diffusion barrier for product gases. The volume between the *CMC* and the aluminum reactor shell is packed with insulating alumina fibers.

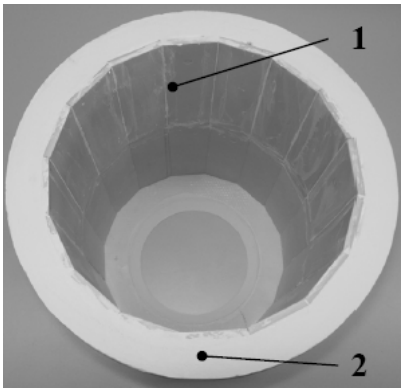

Figure 13: Reactor's cavity made from ZnO tiles (#1) and 80%Al_2O_3-20%SiO_2 insulation (#2). Not seen here are the ZnO tiles on the lateral back and front walls. The cavity's inner diameter is 160 mm and its length is 230 mm. From [54].

1.2. Solar Thermogravimeter (Solar TG)

We have designed and built a versatile tool for testing high-temperature materials and solar reactor components: the solar thermogravimeter (*Solar TG*), shown schematically in Fig. 14. It consists of a solar cavity-receiver, i.e. a well-insulated cylindrical enclosure of 152 mm inner diameter and 150 mm length, lined with 50 mm thick CaO-stabilized ZrO_2 bricks (#1) over two layers of 36 mm thick porous Al_2O_3 (#2). It has a 60 mm diameter aperture for the access of concentrated solar energy through a transparent 3 mm thick quartz window mounted on a water-cooled front (#3). Inside the cavity, a sample holder (#5) is mounted on an Al_2O_3 rod (#6) that is suspended on a balance (#7, *Mettler Toledo*; accuracy 0.01 g). With this arrangement, material samples are directly exposed to concentrated solar radiation, while their weight loss during decomposition is continuously monitored on-line. An Ar flow, injected tangentially and radially at the aperture plane, creates an aerodynamic curtain that protects the window from condensable products and carries the gaseous products Zn(g) and O_2 to the outlet

port (#4) at the rear of the cavity. Ar gas is also introduced into the box containing the balance to prevent back-flow of hot gases. Downstream, the gaseous products are condensed and filtered (glass microfiber filter with pore size of 2.7 µm), and the gas composition is analyzed.

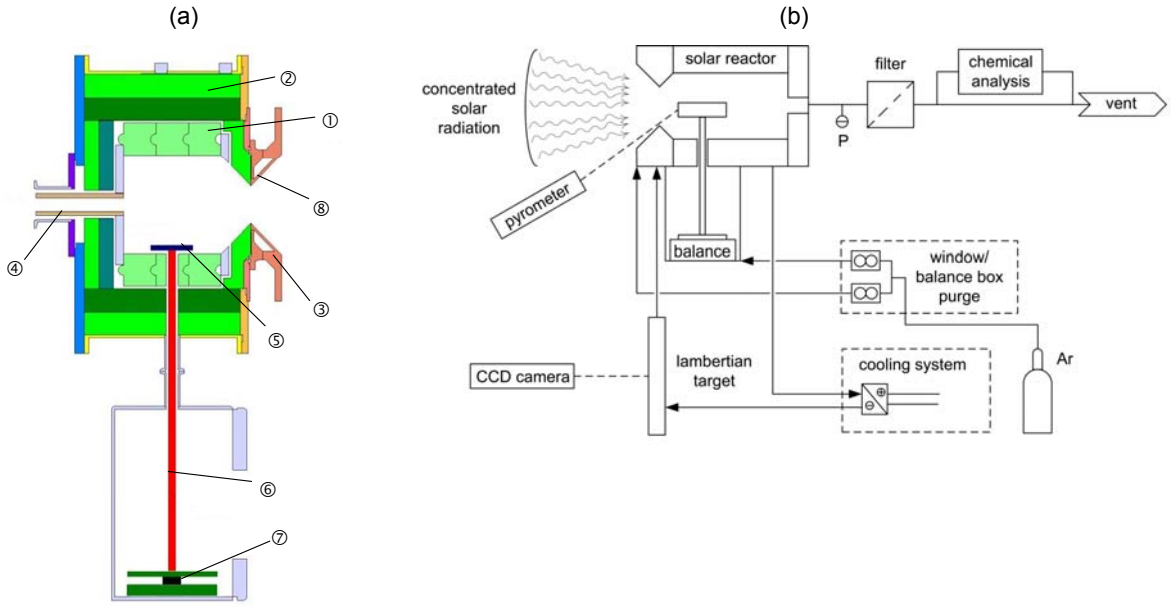

Figure 14: (a) Schematic of solar thermogravimeter (from [59]): 1 = ZrO_2 cavity; 2 = Al_2O_3 insulation; 3 = water cooled front; 4 = gas outlet; 5 = crucible; 6 = balance shaft; 7 = balance; 8 = gas inlet; **(b)** *Solar TG* experimental setup at the solar furnace (from [60]). Material samples are directly exposed to concentrated solar radiation, while their weight loss during the thermal decomposition is continuously monitored.

1.3. Quenching Apparatus

In a parallel development [13],[14], a quenching apparatus was designed, built, and coupled to the *Solar TG*, as shown in Fig. 15. A detailed description is found in a recent publication [56].

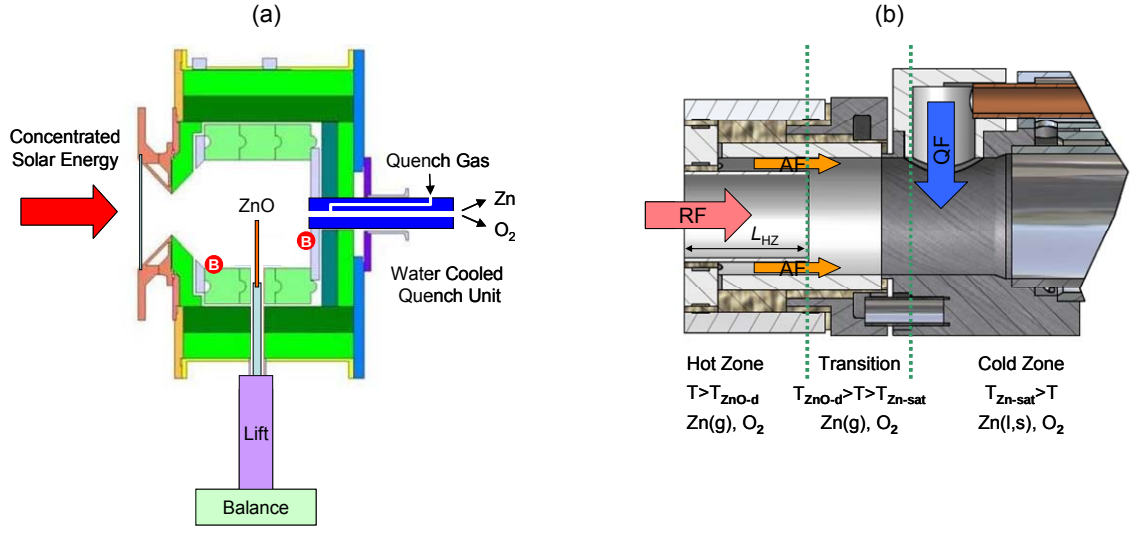

Figure 15: (a) Schematic of the experimental setup with *Solar TG* and quenching apparatus; thermocouples *type B* were used for temperature measurement; **(b)** Schematic of the quenching apparatus illustrating the three temperature zones (*RF*: reacting flow of Zn(g) and O_2 in carrier gas Ar; *AF*: annular flow; *QF*: quench flow; L_{HZ}: hot zone of variable length). From [56].

The quenching apparatus, shown in Fig. 15b, was designed to impede the recombination of the products Zn(g) and O_2 (reacting flow *RF*) resulting from the solar thermal dissociation of ZnO. It features three zones: (1) an inlet hot zone, incorporated at the exit of the solar reactor, where the wall tempera-

ture is kept above the ZnO dissociation temperature $T_{ZnO\text{-}d}$ (> 1700 K); (2) a transition zone at above the Zn(g) saturation temperature $T_{Zn\text{-}sat}$ (820 K for the given experimental conditions), where an annular flow (*AF*) of Ar impedes Zn(g)/O_2 diffusion to the walls; and (3) an outlet cold zone with water-cooled walls, where the injection of cold Ar gas (quench flow *QF*) sharply decreases temperatures below the Zn melting point (693 K) and slows the oxidation kinetics. The hot and transition zones have been realized by a set of three concentric Al_2O_3 tubes. The cold zone consists of a water-cooled stainless steel tube containing a port for the injection of cold Ar.

2. SOLAR EXPERIMENTATION

2.1. Experimental Setup of ZnO Decomposition Reactor

Experimentation with the ZnO decomposition reactor *ZIRRUS* was carried out at *PSI*'s High-Flux Solar Simulator (*HFSS*) [20]. This unique research facility comprises an array of ten high-pressure Xenon arcs (15 kW_e each), close-coupled with truncated ellipsoidal specular reflectors of common focus, and provides an external source of intense thermal radiation (radiative power > 50 kW, radiative power flux > 11,000 kW/m^2) that closely approximates the heat transfer characteristics of highly concentrating solar systems, such as solar towers and solar furnaces; yet it enables experimental work under controlled steady and unsteady conditions for reproducible measurements and model validation. The experimental setup of the 10 kW reactor prototype with peripherals is schematically depicted in Fig. 16.

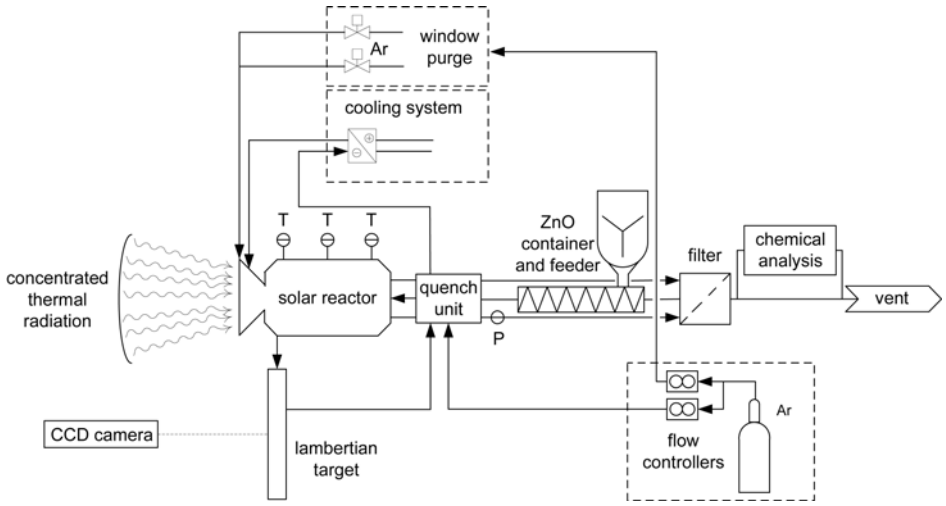

Figure 16: Experimental setup of 10 kW reactor prototype and peripherals at *PSI*'s High Flux Solar Simulator. From [55].

Figure 17 shows a picture of the *ZIRRUS* reactor mounted on the experimental platform of the *HFSS*. Power fluxes incident on the reactor were measured optically with a calibrated *CCD* camera on a water-cooled Al_2O_3 plasma coated *Lambertian* target. Radiation power input into the reactor was calculated by numerically integrating the radiative flux over the reactor's aperture and accounting for the window's mean transmissivity of 93%. Particles formed were collected downstream along the walls of the quench unit and in a filter. After termination of each experiment, solid products were analyzed by *X-ray* diffraction with an accuracy of 7% (*XRD*, *Philips Xpert*, FeK α, λ = 1.93740 Å). The composition of the product gases was analyzed by gas chromatography (*Agilent High Speed Micro GC G2890A*, equipped with molecular sieve 5A and *HaySep A* capillary columns), by *IR*-based detectors for CO and CO_2 (*Siemens Ultramat 23*), and by thermal conductivity-based detector for O_2 (*Siemens Oxymat 6*). The *GC* has a 10 ppm detection limit at a sampling interval of 180 s. The *IR* detector has detection limits of 0.2% for CO and CO_2, at a sampling rate of 1 s^{-1}. The conductivity-based detectors have a minimum detection limit and accuracy of 50 ppm at a sampling rate of 1 s^{-1}. Both CO and CO_2 were monitored to ensure that ZnO was not reduced carbothermally.

A typical experiment consisted of three phases. Firstly, the reactor's cavity was slowly heated to 1600 K within 50 minutes by igniting stepwise four arcs of the *HFSS* and delivering from 1.6 kW to 6 kW through the reactor's aperture. During this heating phase, the cavity temperature was not allowed to exceed 1630 K in order to prevent the directly irradiated ZnO tiles from dissociating. The predicted ZnO dissociation rate at 1630 K is only 4.8 mg/s [61] and, thus, can be tolerated. In the second phase,

the screw-feeder was extended into the cavity and ZnO particles were spread uniformly on the rotating cavity walls. To avoid overheating of the feeder's cap, the power input from the *HFSS* was interrupted briefly during the feed cycle. Afterwards, radiative power was re-established by six arcs and the cavity temperature was maintained in the range 1807-1907 K. In several experimental runs, the feed cycle was repeated. Finally, the *HFSS* was shut down and the reactor underwent cooling while keeping the Ar flow.

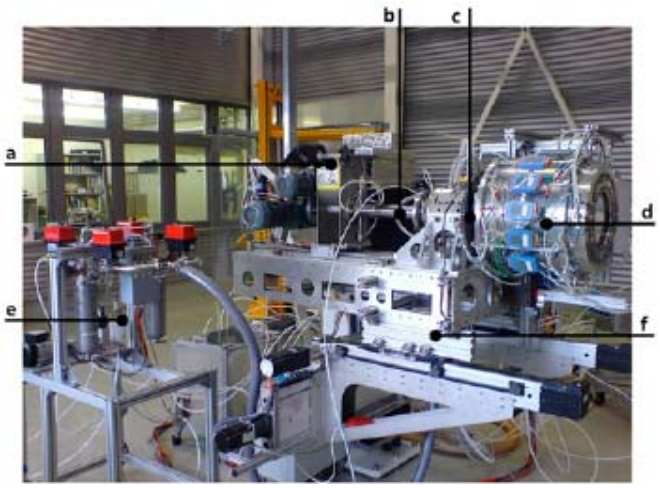

Figure 17: Experimental setup of *ZIRRUS* reactor at *HFSS*: a = ZnO container, b = feeder unit, c = rotary joint, d = rotating reactor, e = filter unit, f = experimental platform. From [62].

2.2. *Results of ZnO Decomposition and Quench Experiments*

A comprehensive description of selected ZnO decomposition experiments conducted at *PSI*'s *HFSS* is found in ref. [54]. Details of quench experiments in the *Solar TG* are given in ref. [56].

ZnO decomposition – Table 1 summarizes the experimental conditions for the cavity lined with 3.7 mm thick ZnO tiles (runs No. 1-8) and with 7 mm thick Al_2O_3 tiles (runs No. 9-11), the latter allowing for higher cavity temperatures [55]. The radiative power input through the reactor's aperture was in the range of 1.2-10.9 kW, with peak concentration ratio of 5800 suns (1 sun = 1 kW/m^2) and maximum mean flux concentration ratio over the aperture of 3860 suns. Mass flow rate of optionally pre-heated Ar (820 K) for keeping the window clean and carrying the gaseous products was in the 0.32-0.49 g/s range. The Ar mass flow rate for quenching the product gases was in the 0.68-2.4 g/s range. The semi-continuous feeding of ZnO ranged from 120 g to 410 g during a feed cycle of typically 50 s. The reactor operated without incident for more than 40 h at maximum temperatures ranging from 1807-1907 K, measured with *type-B* thermocouples behind the sintered ZnO and Al_2O_3 tiles, respectively. Different tile thickness and varying ZnO particle deposition on top of the tiles introduce an uncertainty in the ZnO surface temperature of roughly 20-50 K. Pyrometry was not applied to measure the irradiated ZnO surface temperature because of the intense reflected radiation over a wide spectrum.

Table 1: Operating conditions and results of ZnO decomposition experiments. From [55].

Run No.	# feed cycles	Total ZnO fed (g)	Max. mean radiative flux (kW/m^2)	Max. power input (kW)	ZnO dissociation time (min)	Max. cavity temperature measured behind tiles* (K)	Max. O_2 release (mole/s·10^{-6})	Solid products recovered downstream (g)	Zn content in filtered particles (mole%)
1	1	284	2620	7.4	25	1807	12.8	17.8	18.5 ± 7
2	1	410	3040	8.6	18	1893	22.2	5.2	20.7 ± 7
3	1	398	3040	9.3	48	1862	27.0	25.8	41.7 ± 7
4	2	317	3150	8.9	39	1856	19.1	38.1	33.8 ± 7
5	2	512	3400	9.6	38	1861	18.8	52.3	25.4 ± 7
6=K6	5	600	3190	9.0	64	1907	17.4	66.3	14.6 ± 7
7	7	934	3500	9.9	262	1882	14.1	n.a.	36.1 ± 7
8	9	1180	3320	9.4	241	1880	10.8	292.6	26.7 ± 7
9	2	500	3860	10.9	132	1873	11.2	105.2	34.0 ± 7
10	2	310	3470	9.8	71	1872	27.6	95.1	39.5 ± 7
11	2	339	3470	9.8	73	1858	29.9	93.4	32.3 ± 7

* Runs No. 1-8: cavity lined with ZnO tiles (3.7 mm thick) [54]; Runs No. 9-11: cavity lined with Al_2O_3 tiles (7 mm thick).

Figure 18 shows power input, cavity temperature (measured behind ZnO and Al_2O_3 tiles, respectively), and O_2 molar flow rate in the product gases measured during experimental run No. 8 with 9 feed cycles of 131 g of ZnO each, and during run No. 11 with 2 feed cycles of 170 g of ZnO each, respec-

tively. To avoid overheating of the feeder, the power input was interrupted briefly (~50 s) during each feed cycle. The reactor was operated in so-called “ablation” mode, where the rate of heat transfer – predominantly by radiation – to the thin layer of ZnO particles undergoing endothermic dissociation proceeds faster than the rate of heat transfer – predominantly by conduction – through the cavity walls. The material construction of the cavity fulfilled the rigorous requirements for the reactions. During the experiments, Zn condensation observed on the quartz window did not prevent continuation of the runs.

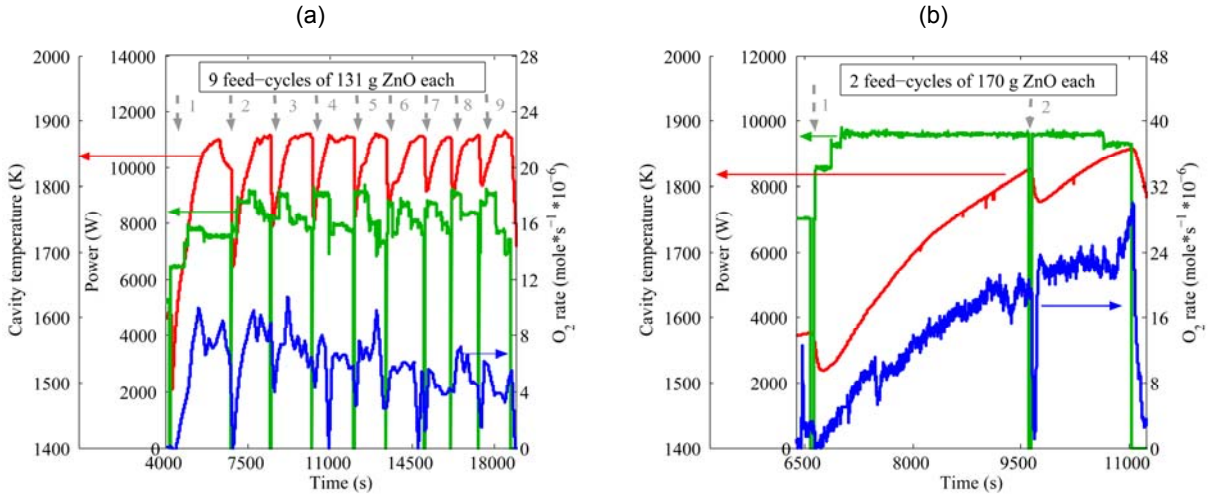

Figure 18: Radiative power input, cavity temperature, and O_2 molar flow rate in the product gases measured during **(a)** run No. 8, with 9 feed cycles of 131 g ZnO each [54]; and **(b)** run No. 11, with 2 feed cycles of 170 g ZnO each. From [55].

For the 11 experiments shown in Table 1, the feed rate of ZnO(s) particles was varied and the level of dissociation was quantified by a mass balance of the entire reactor. The amount of solid products recovered downstream of the cavity’s exit (at the water-cooled surfaces of the quench unit and in the filter; see Fig. 19) represented, in the average, 13% of the total ZnO fed; most of the remainder accumulated inside the cavity and formed a layer on top of the tiles. Some un-reacted as well as recombined ZnO particles agglomerated and were transported downstream of the quench unit. Scanning Electron Microscope (*SEM*) analysis of particles in the filter showed Zn and recombined ZnO only (Fig. 20). The highest Zn content was measured in the filter far downstream; maximum was 41.7 mol% for run No. 3 (Table 1). It correlates well with the amount of O_2 measured at the outlet. In contrast, no correlation was found between the cavity temperatures (measured behind the ZnO and Al_2O_3 tiles) and the oxygen evolution because of varying thickness of the ZnO layer – which in turn affects the temperature – and varying re-oxidation extents of Zn – which in turn affects the O_2 concentration. Part of the continued reactor development work is aimed at optimizing the quench unit configuration for avoiding Zn re-oxidation.

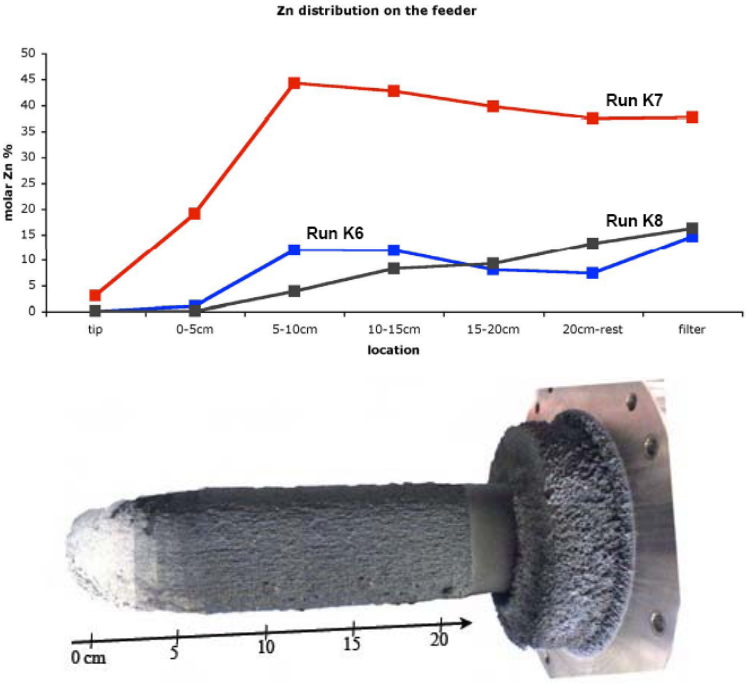

Figure 19: Molar Zn content of recovered products along feeder surface and in filter for runs No. K6 (= No. 6, Table 1), K7, and K8 (**top**). Feeder surface covered with Zn and ZnO particles after experimental run, divided into equal sections of 5 cm length (**bottom**). From [62].

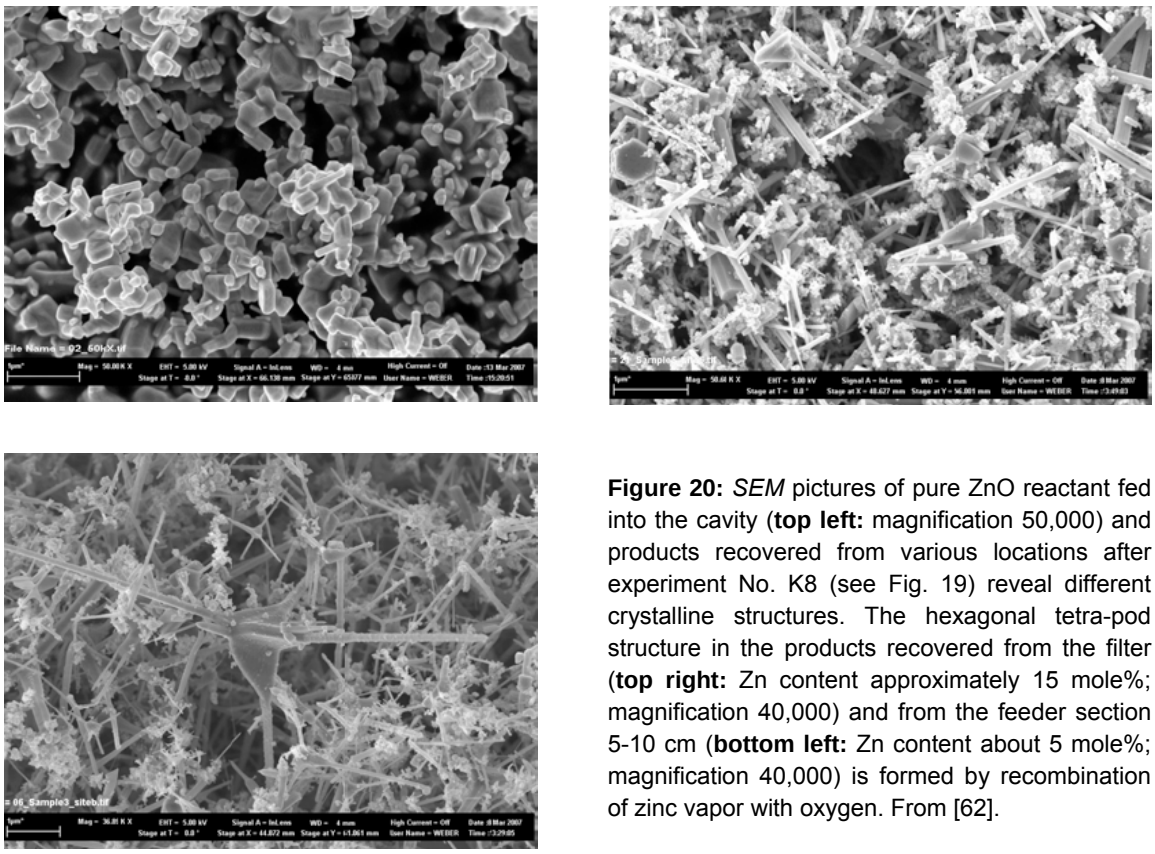

Figure 20: *SEM* pictures of pure ZnO reactant fed into the cavity (**top left:** magnification 50,000) and products recovered from various locations after experiment No. K8 (see Fig. 19) reveal different crystalline structures. The hexagonal tetra-pod structure in the products recovered from the filter (**top right:** Zn content approximately 15 mole%; magnification 40,000) and from the feeder section 5-10 cm (**bottom left:** Zn content about 5 mole%; magnification 40,000) is formed by recombination of zinc vapor with oxygen. From [62].

Figure 21 compares the Zn content of the solid products recovered and determined by *XRD* analysis with the amount of Zn predicted from on-line gas measurements using gas chromatography (*GC*), *Oxymat*, and *Ultramat* during run No. 11 (Table 1). The reactor's mass and gas balances are in good agreement. The observed evolution of hydrogen is attributed to the formation of ZnO(s) and H_2 by hydrolysis of produced Zn(g) or Zn(s) with evaporated moisture that was accumulated in the porous reactor insulation. The oxidized Zn (marked by H_2) is added to the Zn(s) recovered downstream and quantified by *XRD*, thus yielding the total amount of Zn(s) originally formed by the ZnO(s) decomposition reaction. Carbon impurities in the feedstock led to carbothermic production of small amounts of Zn as evidenced by the release of CO and CO_2, which was measured by *Ultramat*, but could not be detected by *GC* due to the short evolution time after each feed-cycle.

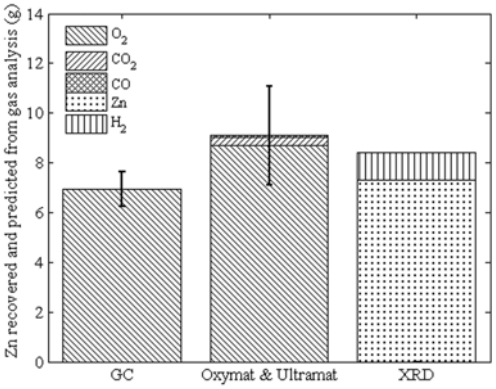

Figure 21: Zn content of solid products recovered and determined by *XRD* analysis (also accounting for partial Zn hydrolysis due to some moisture contained in porous insulation) compared with amount of Zn predicted from on-line gas measurements using *GC*, *Oxymat*, and *Ultramat* during run No. 11 (Table 1). From [55].

Zn/O_2 quench – Rapid cooling for avoiding the recombination of the products Zn(g) and O_2 exiting the solar reactor was investigated using the dedicated solar thermogravimeter (*Solar TG*) coupled to a quenching apparatus [56]. During the experiments, the *Solar TG* was heated up and maintained at a prescribed temperature ranging from 1820 to 2050 K. The nominal cavity temperature was determined by the arithmetic mean value of two shielded thermocouples *type-B* located in the front and rear of the cavity, as indicated in Fig. 15a. A sample of pressed and sintered ZnO was lifted up from the insulation into the hot cavity for direct exposure to concentrated radiation, thus avoiding premature dissociation. Mass flow rate of Ar for keeping the window clean and carrying the gaseous products (Ar in reacting flow *RF*) was in the 0.16-0.24 g/s range. The Ar mass flow rates for the annular flow (*AF*) and for quenching the product gases (*QF*) were in the range 0.06-0.31 g/s and 0.26-0.80 g/s, respectively.

About 3 g ZnO were dissociated in every run. The ZnO dissociation rate was in the range 1.8-15.3 mg/s, which results in molar Ar/Zn(g) dilution for the hot zone (inside the reactor) and cold zone (downstream of *QF* injection) in the range of 30-270 and 170-1500, respectively. As an alternative to dilution, the zinc partial pressure can be defined as

$$p_{Zn} = p_0 \frac{n_{Zn}}{n_{Ar} + n_{Zn} + n_{O_2}} = p_0 \frac{n_{ZnO,dissoicated}}{n_{Ar} + 1.5 \cdot n_{ZnO,dissociated}} \quad (5)$$

where p_0 is the atmospheric pressure and n is the total number of moles of the corresponding species integrated over the duration of the experimental run. Zinc partial pressure in the hot zone (with Ar in reacting flow *RF* only) varied between 400-3000 Pa, while in the cold zone the variation was in the range 70-600 Pa, as the result of injecting Ar in annular flow (*AF*) and quench flow (*QF*), respectively. In some runs, an electric heater was used to preheat the annular flow (*AF*) up to 970 K. Zinc yield, defined as Zn content of the particles collected downstream of *QF* injection, varied in the range 40-94%. Results indicate the technical feasibility of avoiding Zn/O_2 recombination by quenching the gas products in continuous solar processes.

Summary – Figure 22 summarizes and compares experimental results from the *Solar TG* and the ZnO decomposition reactor *ZIRRUS*. In both cases, Zn(s) yield is based on products collected downstream of *QF* injection (taking into account the inaccuracy of *X-ray* diffraction) and depicted as a function of the Zn partial pressure prevailing upstream of *QF* injection. In the case of the *Solar TG*, the uncertainty interval for the Zn partial pressure is a consequence of different approaches to establish the amount of ZnO dissociated, $n_{ZnO,dissociated}$ in Eq. (5). The upper limit is derived from the ZnO weight loss measured on-line with the balance minus ZnO deposits in the hot zone, and the lower limit is determined from particle deposits collected downstream of *QF* injection. Potential dilution of *RF* with *AF* is neglected, but this rough assumption requires confirmation by *CFD*. Ellipses encompass experiments with similar cooling rates of the quench process derived from *CFD* simulations [63], illustrating the trend to higher Zn yield for decreasing Zn partial pressure and increasing cooling rates, as discussed in ref. [56].

For comparison, three data points (No. 9-11, Table 1) from ZnO decomposition experiments with the solar chemical reactor are included in Fig. 22. In this case, both Zn(s) yield and Zn partial pressure are based on solid products collected downstream of *QF* injection. The uncertainty intervals account for un-reacted particles found in the product samples collected upstream the filter. Zinc yield varied in the 16-18% range for Zn partial pressures between 900 and 2100 Pa, which is considerably lower than comparable *Solar TG* results. On the one hand, there is evidence that the non-optimized quench unit coupled to the ZnO decomposition reactor does not allow effective cooling since doubling or even tripling the quench flow – hence increasing the cooling rate – did not show any effect on the Zn yield. On the other hand, assuming at least partial mixing of *AF* and *RF* in the hot zone of the solar thermogravimeter's quenching apparatus would favor higher zinc yield by increasing Ar/Zn(g) dilution, thus shifting the *Solar TG* data points toward lower Zn partial pressure. As a consequence, higher Zn yield would primarily be achieved by increasing the dilution of the reacting flow in the reactor rather than by augmenting the cooling rate at the quench site [64]. Future work aims at increasing the zinc yield by incorporating an optimized

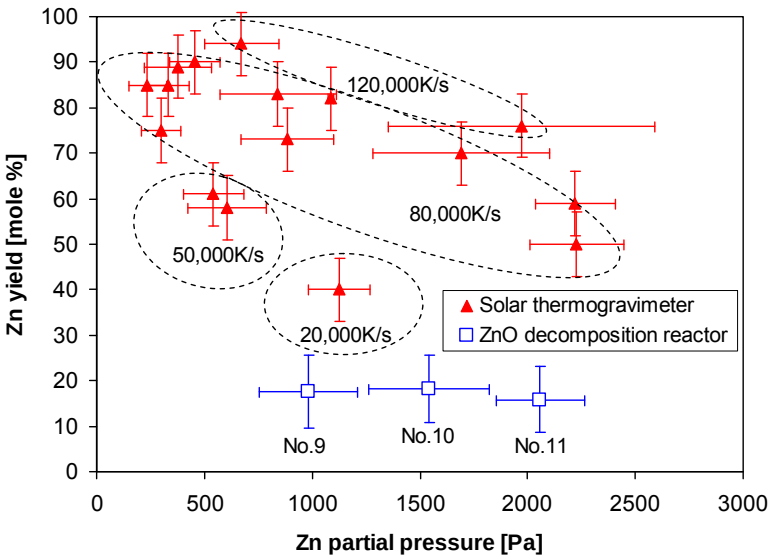

Figure 22: Zinc yield of products collected downstream of *QF* injection vs. zinc partial pressure upstream of *QF* injection for both the solar thermogravimeter [56] and the ZnO decomposition reactor (experimental runs No. 9-11). Ellipses encompass experiments with similar cooling rates derived from *CFD* simulations. From [55].

quench unit at the exit of the ZnO decomposition reactor based on the quench apparatus successfully tested in the *Solar TG*.

Our current understanding of the reaction mechanism is based on both experimental observations [54]-[56] and theoretical considerations [65]. As expected, the ZnO decomposition rate increases with temperature due to enhanced reaction kinetics. Augmented ZnO decomposition, in turn, increases Zn partial pressure in the reactor, favoring recombination of Zn(g) and O_2. This counteracting effect reduces Zn(s) yield, as illustrated in Fig. 22. Obviously, the Zn yield can be increased by diluting the Zn(g)/O_2 mixture with Ar carrier gas in the reaction chamber, thus suppressing recombination of the gaseous products. From Fig. 22, one can also observe a trend to higher Zn yield for higher cooling rates, preferably achieved by increasing the amount of cold quench gas injected at the quench site.

2.3. Materials Testing

High temperature materials were investigated in the special solar thermogravimeter (*Solar TG*), shown in Fig. 23. The reactor cavity has a self-supporting structure made from CaO-stabilized ZrO_2 bricks with low thermal conductivity and nominal operation temperature of 2300 K in inert atmosphere. Two layers of Al_2O_3 insulation are employed, the inner rated to 2100 K, the outer to 1500 K. An interchangeable crucible made from Al_2O_3 is mounted on a ceramic Al_2O_3 shaft and connected to a balance placed beneath the cavity.

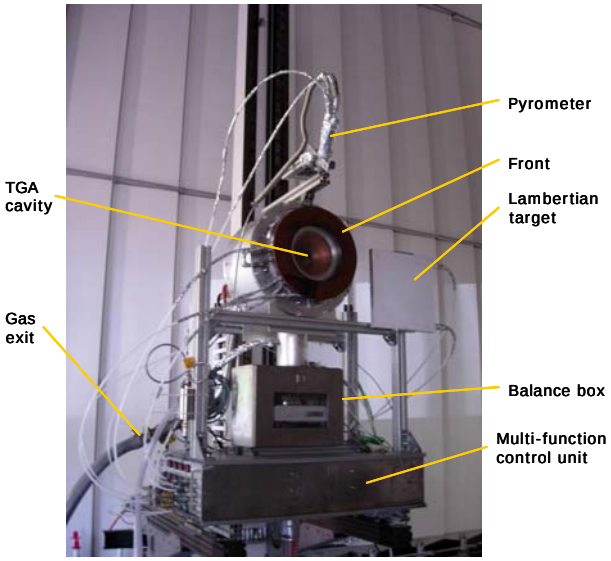

Figure 23: *Solar TG* mounted on the experimental platform at *PSI*'s Solar Furnace. From [59].

The experiments were performed at both *PSI*'s High-Flux Solar Furnace [19] and High-Flux Solar Simulator [20]. Among the most promising materials tested were stabilized ZrO_2 bricks, porous Al_2O_3 insulation and Al_2O_3 ceramic matrix composite (*CMC*) [59]. The experiments were conducted in a protective Ar atmosphere. The samples in contact with sintered ZnO tiles or ZnO powder were exposed to concentrated sunlight for periods up to 30 minutes at maximum temperatures of 2030 K and analyzed by *XRD* and *SEM*. The examined ZrO_2 samples in contact with ZnO exhibited strong surface erosion in the temperature range 1720-2070 K, in contrast to previous findings [66]. All Al_2O_3 samples showed good thermal shock resistance, but the melting point was reduced for the porous 80%Al_2O_3-20%SiO_2 insulation to 1930-1950 K by the eutectic phase of the system ZnO-Al_2O_3-SiO_2 [58]. The 95%Al_2O_3-5%Y_2O_3 ceramic matrix composite (*CMC*) also showed a eutectic phase with ZnO, but at somewhat higher temperatures of roughly 2030 K [59].

2.4. Kinetic Study

In the framework of the ongoing Ph.D. Thesis of L. Schunk [67], an experimental investigation using the solar-driven thermogravimeter (*Solar TG*) for the determination of the ZnO dissociation kinetics was carried out [60]. A packed bed of ZnO particles was directly exposed to concentrated solar radiation at a peak solar concentration ratio of 2400 suns while its weight loss was continuously monitored; the thermal dissociation rate was measured in a setup closely approximating the heat and mass transfer characteristics of solar reactors.

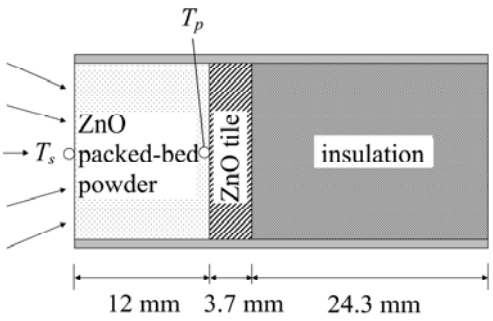

Figure 24: Schematic of sample used in the *solar TG*. Indicated is the location of the temperature measurements: T_p of the ZnO tile is measured by a *type-B* thermocouple, and T_s of the irradiated front surface of the ZnO packed-bed powder is measured by a solar-blind pyrometer. From [60].

The sample investigated is depicted in Fig. 24. It consists of an Al_2O_3 tube (20 mm inner diameter, 40 mm length) containing the same multi-layer arrangement of the solar reactor [54]: a 12 mm thick packed-bed of ZnO powder, followed by a

3.7 mm thick sintered ZnO tile and a 24 mm thick 80%Al_2O_3-20%SiO_2 porous insulation. The total mass of ZnO powder was 6.2 g, with an average porosity of 70.3% ± 0.4%. The temperature of the ZnO tile, T_p, was measured with a *type-B* thermocouple. The temperature of the irradiated front surface of the ZnO packed-bed powder, T_s, was measured by a solar-blind pyrometer.

At *PSI*'s High-Flux Solar Furnace [19], isothermal thermogravimetric runs were performed in the range 1834-2109 K (Table 2). The ZnO surface temperature and sample weight loss as a function of time are shown in Fig. 25 during a representative *Solar TG* run (No. 6). The ZnO surface was heated to 1300 K at a rate of 150 K/s once exposed to a mean solar concentration of 1400 suns, and further heated to 2038 K at a rate of 20 K/s. Measurable weight loss was detected at above about 1825 K (t = 30 s) and continued at a constant rate until the shutter was closed and the run terminated.

Table 2: Summary of solar experimental runs: mean effective surface temperature T_s, mass loss of the ZnO batch Δm during the period of evaluation of length Δt, associated mass loss rate dm/dt per unit of effective surface area, total fractional conversion α_{max}, and normalized linear regression coefficient of the fitted mass loss curve. From [60].

Run No.	T_s (K)	Δm (mg)	Δt (s)	dm/dt (kg/m^2/s)	α_{max} (-)	R^2 (-)
1	2109.1	380	140	0.0176	0.125	0.997
2	1977.8	90	170	0.0034	0.024	0.968
3	1889.8	80	250	0.0021	0.016	0.982
4	1902.1	70	250	0.0018	0.027	0.977
5	1833.6	30	300	0.0006	0.010	0.832
6	2038.6	330	300	0.0071	0.061	0.998
7	1945.6	110	280	0.0025	0.021	0.988

T_s and dm/dt listed in Table 2 were used in the *Arrhenius* plot of Fig. 26. Applying a zero-order rate equation for linear advance of the interface in a single direction [68], the rate law is given in terms of the mass loss per unit of effective (irradiated) surface area as

$$\frac{dm}{dt} = k_0 \exp\left(-\frac{E_a}{RT_s}\right) \tag{6}$$

The corresponding apparent activation energy E_a = 361 ± 53 kJ/mol and frequency factor k_0 = 14.03·10^6 ± 2.73·10^6 kg/m^2/s, each at 95% confidence, were extracted by linear regression. The uncertainty bounds are mainly due to the emissivity value and the balance resolution.

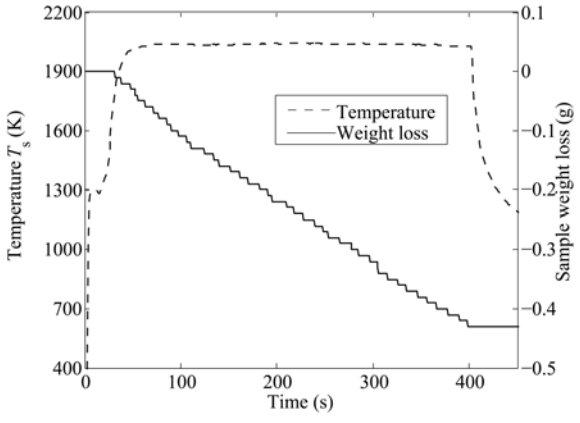

Figure 25: Irradiated surface temperature and weight loss of the ZnO packed-bed powder as a function of time during a representative *Solar TG* run (No. 6, Table 2). From [60].

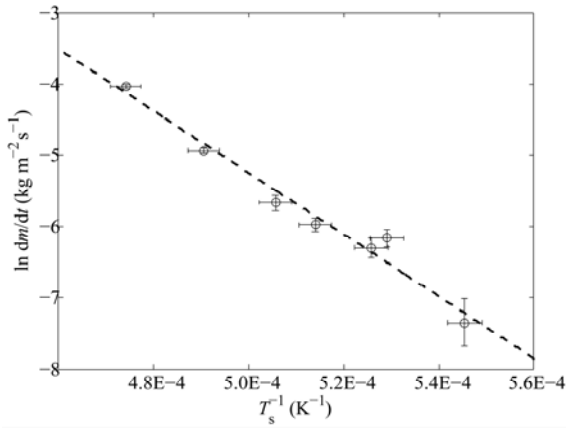

Figure 26: *Arrhenius* plot for the rate law, Eq. (6). Uncertainty bounds of experimental data (circles) are mainly due to the emissivity value and the balance resolution. From [60].

Application of *L'vov*'s kinetic expression [69] for solid decomposition along with a convective mass transport correlation yielded kinetic parameters in close agreement with those derived from experi-

mental data. Sintering was observed prior to ZnO dissociation. The packed bed of ZnO powder was subjected to a transient ablation regime characterized by a rate of radiative heat transfer to the top layer of ZnO packed bed undergoing endothermic dissociation that proceeded faster than the rate of conductive heat transfer to the depth of the packed bed.

3. REACTOR MODELING

3.1. Transient Heat Transfer – "Ablation" Model

In the framework of the ongoing Ph.D. Thesis of L. Schunk [67], a *1D* transient thermal model was developed for simulating an irradiated packed-bed of ZnO particles undergoing sintering and thermal decomposition. The governing equations that couple the heat transfer rate to the decomposition reaction were formulated along with sintering and boundary conditions. Validation was accomplished for the ZnO surface and bed temperatures by comparing numerically calculated values with experimental results [60] obtained from runs in a solar-driven thermogravimeter (*Solar TG*) in *PSI*'s High-Flux Solar Furnace [19].

We present preliminary results of work in progress (journal publication in preparation [70]). As an example, Figures 27 and 28 show measured and modeled T_s, T_p, and the sample weight loss for runs 2 and 3, respectively, of experimental data presented in [60] (see Table 2). The initial effect of 1% of the packed-bed ZnO powder weight was isolated to the first heating stage of run No. 2 (Fig. 27) at temperatures in the order of 1200 K. Measured and modeled temperatures rapidly increased at t = 360 s due to a step-wise increase of the incident solar radiation flux of 1.22 MW/m^2 resulting in an increase of T_s to a stationary temperature of about 1950 K. Since the initial effect occurred prior to the increase in radiation flux, close agreement of measured and modeled sample weight loss is obtained where the concave profile of T_s in the range 360 s < t < 440 s result in a convex mass loss profile. Modeled and measured T_s and weight loss agree well, whereas modeled and measured T_p show minor discrepancy and was attributed to complex change of thermal conductivity in the packed bed of ZnO powder undergoing rapid sintering along with the formation of small cracks. Good agreement of measured and modeled T_s and weight loss was also found in run No. 3 shown in Fig. 28 where the packed bed of ZnO powder was subjected to a step input of solar radiation flux at 1.177 MW/m^2. The small dip of T_s at t ~ 80 s is ascribed to the formation of a small crack on the illuminated sample surface, corroborated by *CCD* camera pictures. The second dip of T_s at t ~ 220 s with subsequent temperature increase was due to a decrease of incident radiation flux followed by a slight increase.

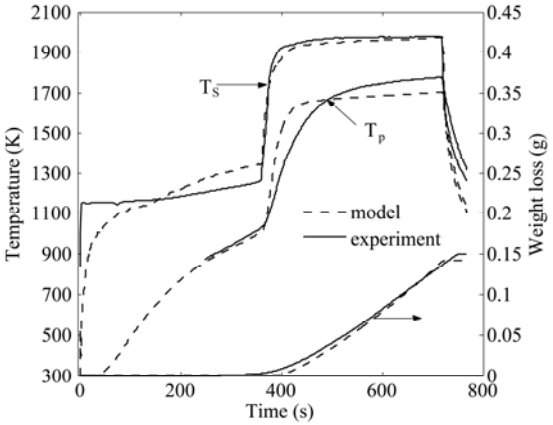

Figure 27: Measured and calculated T_s, T_p, and weight loss of the ZnO batch vs. time for run No. 2 (see Table 2, [60]). From [70].

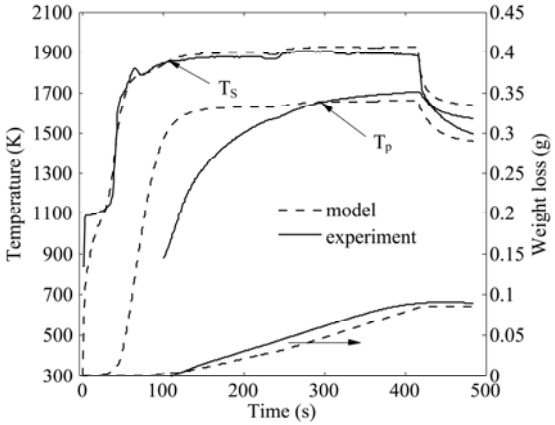

Figure 28: Measured and calculated T_s, T_p, and weight loss of the ZnO batch vs. time for run No. 3 (see Table 2, [60]). From [70].

SEM pictures of the packed bed of ZnO particle reveal a structure of grain sizes in the range of 2-12 µm and pores with diameters in the range 0.3-0.8 µm (Fig. 29). The active layer of dissociation was about 1.0 mm thick and corresponds approximately to the layer thickness of needles and ridges which were observed in the sample after the experiment (Fig. 30). All seven runs from the previous experimental study [60] were modeled and good agreement was found regarding surface temperature T_s and dissociation rate.

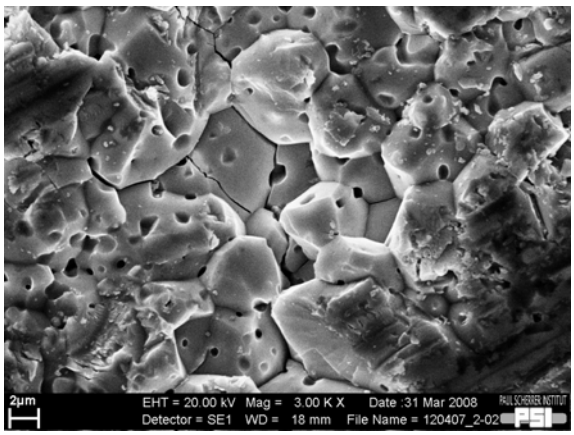

Figure 29: Cross section of the sintered ZnO batch of sample depicted in Fig. 24. Grain sizes are in the range 2-12 µm, pore diameters are in the range 0.3-0.8 µm. From [70].

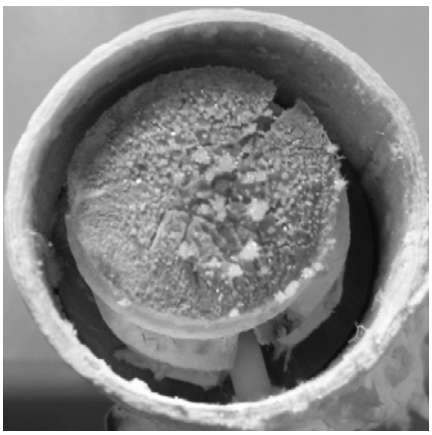

Figure 30: Sintered ZnO sample after illumination in the *Solar TG*. The ablated surface region is characterized by small cracks, needles and ridges. From [70].

3.2. Transient Heat Transfer – Reactor Model

Modeling of the directly irradiated solar ZnO decomposition reactor *ZIRRUS* requires matching the rate of heat transfer to the rate of chemical reaction. Within the framework of the ongoing Ph.D. Thesis of L. Schunk [67], a transient solar chemical reactor model coupling combined radiative-conductive-convective heat transfer with endothermic dissociation of ZnO was formulated and solved numerically using the explicit Euler method. Radiative heat transfer was modeled in *3D* employing the *Monte Carlo* (*MC*) ray tracing method for incident radiation from the *HFSS* arcs along with the radiosity method for radiative heat exchange between interior surfaces. Conductive, convective, and chemical heat flows were modeled in a *2D* axisymmetric domain using the finite volume technique.

We present preliminary results of work in progress (journal publication in preparation [71]). The transient thermal model is formulated for the solar reactor depicted in Fig. 11. The unsteady-state energy conservation equation is given by

$$\rho c_p \frac{\partial T}{\partial t} = \nabla\left(k_{eff} \nabla T\right) + q''' \tag{7}$$

Boundary and initial conditions for Eq. (7) are given

- at internal surfaces: $$k\nabla T \cdot \hat{n} = h_{\text{int}}\left(T - T_{gas}\right) - q''_{r,\text{int}} + q'' \tag{8}$$
- at external surfaces: $$k\nabla T \cdot \hat{n} = h_{ext}\left(T_{amb} - T\right) \tag{9}$$
- initial conditions: $$T\left(x, r, t = 0\right) = T_0 \tag{10}$$

The effective thermal conductivity of ZnO in Eq. (7) is given by

$$k_{eff} = k + k_r\,, \qquad k_r = \frac{16n^2}{3\beta_r}\sigma T^3 \tag{11}$$

where k_r corresponds to the *Rosseland*'s diffusion approximation. The term q''' in Eq. (7) is the volumetric heat sink due to the endothermic dissociation of ZnO. The ZnO decomposition rate is linked to the actual composition of the solid phase which is obtained by solving a transient mass conservation equation

$$r_{ZnO} = \frac{dn_{ZnO}}{dVdt} \tag{12}$$

where *dV* is a differential volume of ZnO shrinking with time as the sample undergoes sintering. The ZnO decomposition rate is modeled by applying a zero-order *Arrhenius*-type rate law according to [60]

$$r_{ZnO} = ak_0 \exp\left(-\frac{E_a}{RT_s}\right) \tag{13}$$

with the specific surface area *a*; the kinetic parameters k_0 = 172.13·10^6 mol/m^2/s and E_a = 361 kJ/mol have been experimentally determined for ZnO samples directly irradiated at *PSI*'s solar furnace [19]. The convective heat flow at the internal surfaces, $h_{int}\ (T\text{-}T_{gas})$ in Eq. (8), was estimated by performing *CFD* simulations of the internal gas flow inside the reactor, resulting in values between 150 W/m^2 and 1350 W/m^2. The external convective heat transfer coefficient h_{ext} in Eq. (9) was approximated for heat transfer from the aluminum reactor shell, resulting in 3 W/m^2 for angular velocity of 0.5 s^{-1} and characteristic length of 0.4 m (reactor's diameter). At the window, h_{ext} was modeled via a combined *Nu* number accounting for free convection from a vertical plate [72] and forced convection due to the reactor rotation (correlation for a spinning disk [73]).

Radiative exchange at internal surface elements A_i was modeled by applying the radiosity method [74] for calculating the incoming and outgoing radiative fluxes $q''_{i,j}$ and $q''_{o,j}$, respectively:

$$q''_{r,\mathrm{int},j} = q''_{i,j} - q''_{o,j} + q''_{solar} \tag{14}$$

The distribution of the solar flux q''_{solar} at the interior surfaces was computed by the *MC* method for the optical characteristics of the *HFSS* facility [20],[75]. The incident solar heat flux was calibrated with the radiative power measured calorimetrically at the aperture opening behind the quartz window (transmissivity ~93% before experiment). The configuration factors were calculated by *MC* with 10^8 rays emitted from each surface. The frustum and cavity walls were modeled as diffuse surfaces and were divided into conical, cylindrical, and annular elements. The window at the reactor's frustum was divided into annular elements and treated transparent for incident radiation and grey diffuse absorbing and emitting in the infrared wavelength range. Radiative exchange between the outer reactor mantle and the ambience was neglected because of bulky thermal insulation.

A representative experimental run with three feed cycles of 103 g ZnO each was used to validate the reactor model. Prior to the first feed cycle of ZnO powder, the reactor was heated up by step-wise ignition of the Xenon arcs to about 1600 K measured at location $T_{B,1}$ at the backside of the cavity tiles, as indicated in Fig. 31. Measured center temperature $T_{B,1}$ and incident radiative power across the aperture along with measured O_2 from ZnO dissociation are shown in Fig. 32 in the time period ranging from the first feed cycle to the extinction of the arcs. The power input was interrupted for ~40 s during the first feed cycle resulting in a temperature drop of 50 K. As soon as the power input was re-established, the temperature started to rise and dissociation of ZnO occurred as indicated by the O_2 measurement. Note that a substantial portion of the O_2 formed by ZnO dissociation recombined with Zn(g), as determined by the ZnO mass balance.

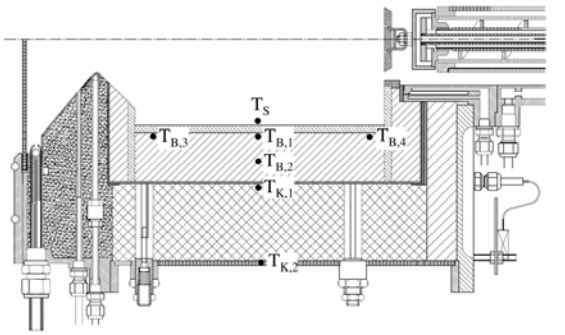

Figure 31: Cross section of the solar chemical reactor (Fig. 11) with window (left) and feeder (upper right). Indicated are the locations of temperature measurements with *type-B* (B) and *type-K* (K) thermocouples. From [71].

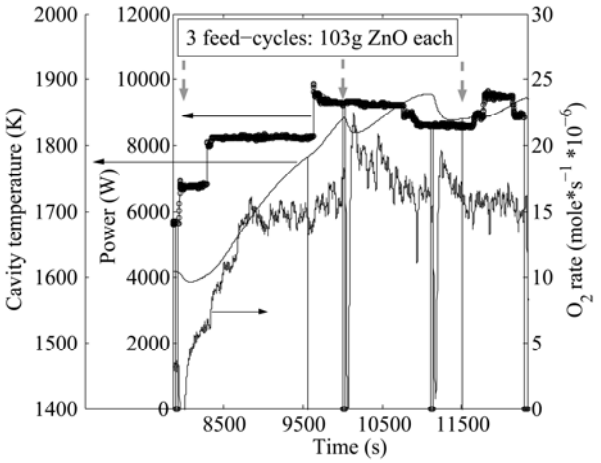

Figure 32: Radiation power input, center temperature $T_{B,1}$ (Fig. 31), and O_2 molar flow rate in the product gases measured during a representative experimental run with three feed cycles of 103 g ZnO each. From [71].

Figure 33 depicts temperatures $T_{B,1}$, $T_{B,2}$, $T_{K,1}$, $T_{K,2}$ measured and modeled across the cavity wall and insulation, as well as the modeled temperature of the irradiated cavity surface T_s. The agreement of all

measured and modeled temperatures is excellent above 1500 K with absolute deviations of less than 30 K. Larger discrepancies are found for temperatures below 1500 K; they are ascribed to uncertainties in thermal conductivity and density of the materials of construction. The temperature gradient across the irradiated ZnO surface layer and the backside of the cavity tiles is maximal 43 K (T_s-$T_{B,1}$), resulting from the relatively high thermal conductivity of both sintered ZnO layer and Al_2O_3 tiles. During the first feed cycle, the surface temperature T_s drops close to room temperature shortly after feeding cold ZnO powder, before rapidly recovering to the original temperature due to high heating rates resulting from the hot cavity tiles and incident radiative power. In subsequent feed cycles, the observed temperature drop of T_s was less pronounced, presumably due to perfect and instant mixing of hot ZnO from previous feed cycles and fresh cold ZnO powder.

Temperatures measured and modeled behind the Al_2O_3 tiles at the front and rear end of the cavity show excellent agreement for temperatures exceeding 1500 K (Fig. 34). The inset of Fig. 34 depicts the high temperature range for the time period 7500 s < t < 12600 s. The model assuming of instant ZnO feeding results in faster temperature drop and subsequent temperature rise compared to the measured temperatures since the actual duration of the feed cycle in the experiment was ~40 s.

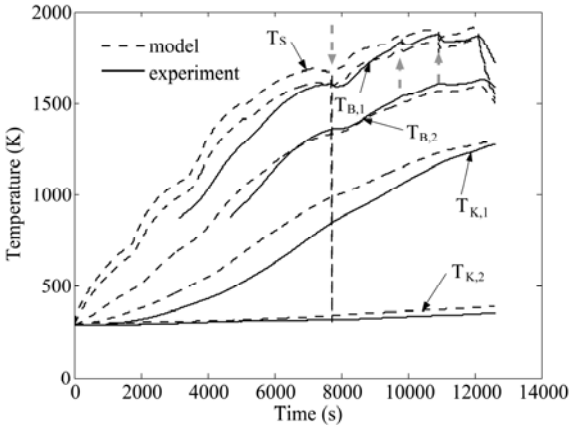

Figure 33: Modeled and measured temperatures halfway along the reactor cavity wall. Note that temperatures measured with *type-B* thermocouples are plotted only in their valid measurement range from 873 K to 2093 K. Feeding of ZnO is indicated by the grey arrows. From [71].

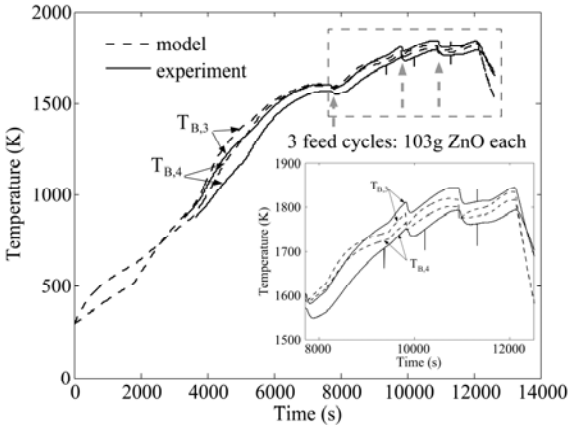

Figure 34: Modeled and measured temperatures $T_{B,3}$, and $T_{B,4}$. Note that temperatures measured with *type-B* thermocouples are plotted only in their valid measurement range from 873 K to 2093 K. Feeding of ZnO is indicated by the grey arrows. From [71].

The model was validated by comparing measured and modeled temperatures at various locations behind the cavity tiles and inside the reactor insulation. Dominant heat losses were found to be due to re-radiation and water-cooled reactor components in the vicinity of the hot cavity tiles. In a final stage, the model is being applied to predict the performance of a reactor scale-up to 100 kW.

3.3. CFD Design of the Reactor's Front – Window Protection

Condensation of gaseous products and deposition of aerosols on the window may deteriorate its transmissivity, resulting in lower reactor efficiency and eventually leading to the destruction of the window. Computational Fluid Dynamics (*CFD*) was employed to determine Ar nozzle locations and orientations for optimum flow configuration of the aerodynamic window protection [76],[77]. *ANSYS CFX* [78] code was used to solve the governing 3-dimensional *Navier-Stokes* equations for simulating the flow patterns akin to the natural tornado phenomenon [79]. The quadratic *Reynolds* shear stress turbulence model was applied because it best copes with turbulence effects of rotational flows [80]. Modes of heat transfer considered were convection and conduction. Radiative transfer was omitted for simplification since the emphasis was on obtaining the fluid flow field in the proximity of the window. The boundary wall temperatures applied correspond to the experimentally measured values. The window, frustum, and cavity temperatures were set to 900, 900, and 2000 K, respectively. The rate of ZnO dissociation into Zn(g) and O_2 at 2000 K was set to 0.17 g/s [50]. The optimal flow configuration leading to the lowest concentration of Zn(g) close to the window was obtained by injecting Ar gas through twelve nozzles of 2.5 mm diameter in radial direction at a plane next to the window and through six nozzles of 1.7 mm diameter at an angle of 45° with respect to the radial direction at the

aperture plane. The Ar mass flow rate through each nozzle was 0.032 g/s at the window and 0.02 g/s at the aperture. Figure 35 shows the velocity field (in m/s) in the central cross section of the reactor for the optimal flow configuration.

Due to the frustum shape of the reactor's front part, eddy flow patterns formed close to the window. These eddies did not extend beyond the aperture and, therefore, did not carry products by convection from the cavity compartment to the window. However, further increase of the Ar flow rate resulted in the breakdown of the vortex flow pattern in the frustum's region, leading to back-flow from the cavity towards the window. Pre-heated Ar gas entered the reactor at 900 K; a mixture of Ar and product gases Zn(g) and O_2 exited the reactor at 1350 K. The gas temperature increase resulted from convective heat transfer between fluid and cavity walls and from the generation of Zn(g) and O_2 at 2000 K. The Zn(g) concentration in the reactor is shown in Fig. 36. The Zn(g) mole fraction was in the range $7 \cdot 10^{-6}$ to $18 \cdot 10^{-6}$ at the plane located 4 mm from the window, and in the range 0.01 to 0.66 inside the cavity.

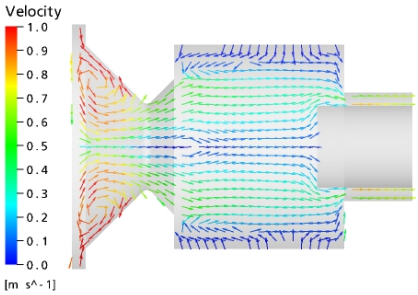

Figure 35: Velocity field in the central cross section of the reactor. From [76].

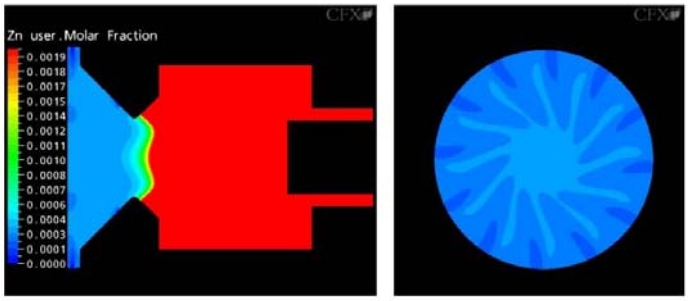

Figure 36: Zn(g) mole fraction in the reactor (left) and in a plane 4 mm from the window (right). From [76].

Although we have been able to operate the ZnO decomposition reactor, at times for hours, we still do not have a fundamental enough understanding of the diffusion and convective flow processes to develop a window design that will work under any circumstances. Work is in progress.

Nationale Zusammenarbeit – National Cooperation

The Solar Technology Laboratory at *PSI* is working jointly with the Professorship in Renewable Energy Carriers at *ETH Zürich*.

National cooperation is performed within the framework of

- Swiss *Competence Center Energy and Mobility (CCEM-CH)*
- *Hydropole – Swiss Hydrogen Association* (*PSI* Representative: Dr. Christian Wieckert)
- Current collaboration and synergism with other research laboratories:

Switzerland	*ETH* Zürich – Particle Technology Laboratory (Prof. S. Pratsinis)
	EMPA – High Performance Ceramics Laboratory (Dr. U. Vogt)

Internationale Zusammenarbeit – International Cooperation

International cooperation is being performed within the framework of

- *IEA's SolarPACES Implementing Agreement* (Task II – ***Solar Chemistry Research***; Operating Agent: Dr. A. Meier)
- *IEA's Hydrogen Implementing Agreement* (Task 25 – ***High Temperature Hydrogen Production Processes***; Swiss Representative: Dr. A. Meier)
- *IPHE – International Partnership for the Hydrogen Economy* (Project: ***Solar driven high temperature thermochemical production of hydrogen***; Swiss Representative: Prof. Dr. A. Steinfeld)

- *SOLLAB – Alliance of European Laboratories on solar thermal concentrating systems* (Collaboration of five leading European solar research laboratories, namely *CIEMAT*, *CNRS*, *DLR*, *ETH*, and *PSI*; Swiss Representative: Prof. Dr. A. Steinfeld)
- *EU FP7 SOLHYCARB* – Hydrogen from solar thermal energy: high temperature solar chemical reactor for co-production of hydrogen and carbon black from natural gas cracking.
- Current collaboration and synergism with other research laboratories:

Australia	*ANU* – Australian National University, Canberra
	CSIRO – Commonwealth Scientific and Industrial Research Organisation
France	*CNRS* – Centre National de la Rechèrche Scientifique, Odeillo
Germany	*DLR* – Deutsches Zentrum für Luft- und Raumfahrt, Köln/Stuttgart
Israel	*WIS* – Weizmann Institute of Science, Rehovot
Japan	*TIT* – Tokyo Institute of Technology, Tokyo
Spain	*CIEMAT* – Centro de Investigaciones Energéticas, Medioambientales y Tecnológicas
USA	*NREL* – National Renewable Energy Laboratories, Golden, CO
	SNL – Sandia National Laboratory, Albuquerque, NM
	UC – University of Colorado, Boulder, CO

Bewertung - Evaluation

Achievements – A 10 kW receiver-reactor prototype (called *ZIRRUS*) for the solar thermal decomposition of ZnO was further improved and tested. The rotating cylindrical cavity was made of either sintered ZnO or sintered Al_2O_3 tiles placed on top of a multi-layer Al_2O_3-SiO_2-Y_2O_3-based ceramics for thermal shock resistance, mechanical stability, gas diffusion barrier, and thermal insulation. Preheated Ar gas was injected for aerodynamic window protection and for minimizing recombination of product gases in the cavity. Experimentation was carried out at *PSI*'s High-Flux Solar Simulator with the direct heating 10 kW reactor prototype subjected to peak radiative fluxes exceeding 5800 suns. The reactor operated without incident for a total of more than 40 h at maximum temperatures – measured behind the ZnO and Al_2O_3 tiles – ranging from 1807-1907 K. Thermal dissociation of ZnO(s) near 2000 K was demonstrated for experimental runs over 4 h in transient ablation mode with up to nine semi-continuous feed cycles of ZnO particles.

In a parallel development, a quenching apparatus was designed and fabricated for avoiding the recombination of gaseous products Zn(g) and O_2 derived from the solar thermal dissociation of ZnO. Experimentation was performed using a solar thermogravimeter (*Solar TG*) in which samples of ZnO were directly exposed to concentrated solar radiation while their rate of dissociation was monitored online. The exit of the solar thermogravimeter was integrated to the inlet of the quench apparatus. The annular flow protection worked well and eliminated deposits in the transition zone. Zinc yields of up to 94% were obtained when using total Ar/Zn(g) dilution of 530 and a cooling rate of about 10^5 K/s. Quench rates were estimated by Computational Fluid Dynamics (*CFD*). Results indicate the technical feasibility of avoiding Zn/O_2 recombination by quenching the gas products in a continuous solar process.

Compared to the solar thermogravimeter (*Solar TG*) results, the Zn yield in the ZnO decomposition reactor (*ZIRRUS*) was significantly lower, varying in the 16-18% range for Zn partial pressures between 900 and 2100 Pa. Higher Zn yield may be obtained by increasing the Ar/Zn(g) dilution in the reactor cavity or by augmenting the cooling rate at the quench site.

In conclusion, at the end of the current *BFE* projects [1],[13] we have reached a sufficient understanding of the chemical-mechanical engineering science required for scaling up our reactor concept to the level of 100 kW. We have demonstrated that the direct heating 10 kW solar reactor prototype called *ZIRRUS* is capable of effecting the thermal dissociation of ZnO(s) near 2000 K. A working Zn/O_2 separation device based on the rapid quenching of the Zn/O_2 mixture is ready to be incorporated at the exit of the solar reactor. In parallel, the development of a reactor model that couples radiation, conduction, and convection heat transfer to the reaction kinetics will allow determining optimal operational conditions for matching the feeding rate to the reaction rate and for maximizing solar-to-chemical energy conversion efficiency.

Challenges – Although many of the design goals for the solar reactor scale-up have already been reached, the following challenges still remain to be resolved:

(1) *Quench* – The newly developed Zn/O_2 separation device will be integrated into the *ZIRRUS* reactor to optimize the quenching of the products at the exit of the solar reactor. Part of the continued reactor development work is to find an optimal configuration of the transition zone from hot to cold that leads to good Zn yields without compromising the reactor efficiency.

(2) *Inert gas* – An inert gas (Ar or N_2) is swept across the reactor window and through the aperture, carrying the gaseous products Zn(g) and O_2 to the quench zone at the exit of the cavity. The amount of an inert gas should be minimized because of the energy penalty associated with its separation and recycling. Furthermore, the effect of preheating the inert gas to temperatures above 900 K for prevented the formation of Zn droplets and aerosols in the reactor cavity should be investigated in more detail.

(3) *Window protection* – Although we have been able to operate our ZnO decomposition reactor, at times for hours, we still do not have a fundamental enough understanding of the diffusion and convective flow processes to develop a window design that will work under any circumstances. Being able to guarantee a functioning window is a fundamental requirement before scaling up a direct heating reactor.

With regard to the scale-up of the reactor to 100 kW proposed within the follow-up project [81], the integration of a secondary concentrator (*CPC*) into the solar reactor and the inclined reactor operation will be needed only if the planned scale-up takes place at the 2.7 MW solar tower facility of the *Plataforma Solar de Almería, Spain.* However, our preferred option is the 1 MW solar furnace at *CNRS-Odeillo, France*, since there the solar reactor can be operated horizontally and the required solar flux concentration can be achieved without using a *CPC*. Therefore, we consider the following topics as second priority only (*optional*):

(4) *Secondary concentrator (CPC)* – For industrial applications, it is conceivable that a secondary concentrator (*CPC*) has to be mounted in front of the reactor's aperture to ensure sufficient solar flux concentration to reach the required temperatures.

(5) *Mechanical functionality* – The *ZIRRUS* reactor has been tested and modeled receiving sunlight from a horizontal direction; however, an industrial reactor will presumably operate at some angle from the horizontal if it is to be used in a solar tower configuration. There is no experimental experience working with the reactor in such geometrical orientations that are industrially realizable. For example, we will have to ensure that the current mechanical ZnO(s) feeding system will still function reliably and that the window will be protected from deposition of particles and condensable gas.

Within the follow-up project [81], we will further optimize the solar reactor technology for the thermal dissociation of ZnO at the laboratory scale (solar power input of 10 kW) and aim at successfully demonstrating the fully integrated reactor at pilot scale (solar power input of 100 kW). We will develop conceptual designs and preliminary economics for commercial solar Zn production and storage facilities based on large-scale concentrating solar power (*CSP*) tower technology.

The results from this research program will advance our ability to store solar energy as a fuel, such as Zn or hydrogen, in a manner that increases our chances of having a sustainable solution to the current world problem of being dependent on a limited supply of fossil fuels.

Publikationen – Publications under the Current Contract (2005-2007)

The following is a list of publications originating from the current *Solar Zinc Project* [1].

Peer-reviewed Journals

L.O. Schunk, W. Lipiński, A. Steinfeld: ***Transient numerical model of a directly irradiated receiver-reactor for the solar thermal dissociation of zinc oxide***, to be submitted 2008.

L.O. Schunk, W. Lipiński, A. Steinfeld: ***Numerical and Experimental Study on Ablation and Sintering of Zinc Oxide under Direct High-Flux Irradiation***, AIChE Journal, to be submitted 2008.

L.O. Schunk, A. Steinfeld: ***Thermal dissociation kinetics of ZnO exposed to concentrated solar irradiation using a solar-driven thermogravimeter in the range 1800-2100 K***, AIChE Journal, submitted January 2008.

L.O. Schunk, P. Haeberling, S. Wepf, D. Wuillemin, A. Meier, A. Steinfeld: ***A Receiver-Reactor for the Solar Thermal Dissociation of Zinc Oxide***, *J. Sol. Energy Eng.* 130 (2), 021009, 2008.

Ph.D. Thesis

L.O. Schunk: ***Solar Thermal Dissociation of Zinc Oxide: High-Temperature Receiver-Reactor Modeling and Experimentation***, ETH Zürich, Switzerland, to be submitted 2008.

Bachelor / Diploma / Master Theses

M. Schmid: ***Solar experimental investigation of a solar reactor for ZnO dissociation***, Bachelor Thesis, PSI Villigen and ETH Zürich, 2005.

S. Meder: ***Modification of test reactor SOLAR-TG and accomplishment of material tests***, Bachelor Thesis, PSI Villigen and ETH Zürich, 2005.

P. Leu: ***Untersuchung einer Tornado-Gasführung im ZIRRUS Solarreaktor mit CFD***, Master Thesis, PSI Villigen and ETH Zürich, 2006.

V. Gianini: ***Solar Thermogravimetric Material Tests for a Solar Reactor***, Bachelor Thesis, PSI Villigen and ETH Zürich, 2006.

N. Rotering: ***Investigation of the decomposition rate of ZnO particles under direct solar irradiation in a solar thermogravimeter***, Bachelor Thesis, PSI Villigen and ETH Zürich, July 2007.

P. Vielle: ***Heliostat field calculations of central receiver systems for hydrogen production using the ZnO/Zn cycle and Life cycle assessment on solar steam-gasification of carbonaceous materials***, Master Thesis, PSI Villigen and ETH Zürich, October 2007.

C. Suter: ***Development and experimental investigation of a quench unit for a solar thermal rotary reactor***, Master Thesis, PSI Villigen and ETH Zürich, April 2008.

Semester Theses

D. Kronenberg: ***Experimental investigation of the solar thermal dissociation of ZnO in a rotary reactor***, Semester Thesis, PSI Villigen and ETH Zürich, March 2007.

C. Suter: ***CFD Modeling of a Solar Reactor for the Thermal Decomposition of Zinc Oxide***, Semester Thesis, PSI Villigen and ETH Zürich, July 2007.

Conference Proceedings

L.O. Schunk, D. Gstoehl, A. Meier, A. Steinfeld: ***Technological advances toward scale-up of solar chemical reactor for thermal ZnO decomposition***, *Proc. 14th International Biennial SolarPACES Concentrating Solar Power Symposium*, Las Vegas, Nevada, USA, March 4-7, 2008.

L.O. Schunk, P. Haeberling, S. Wepf, D. Wuillemin, A. Meier, A. Steinfeld: ***A Rotary Receiver-Reactor for the Solar Thermal Dissociation of Zinc Oxide****, Proc. ES2007, Energy Sustainability 2007*, Long Beach, California, USA, June 27-30, 2007.

R. Müller, L. Schunk, A. Meier, A. Steinfeld: ***Solar Thermal Dissociation of Zinc Oxide in a Directly-Irradiated Rotary Reactor***, *Proc. 13th SolarPACES International Symposium*, Seville, Spain, June 20-23, 2006.

PSI Scientific Reports

L.O. Schunk, D. Gstöhl, P. Häberling, D. Wuillemin, A. Meier, A. Steinfeld: ***Technological advances in the two-step H_2O-splitting thermochemical cycle***, *PSI Scientific Report 2007*, pp. 32-33, 2008.

Invited Talks

A. Steinfeld: ***The ZnO/Zn water-splitting thermochemical cycle****, Solar Colloquium*, DLR-German Aerospace Center, June 14, 2005.

D. Gstoehl, A. Steinfeld: ***Solar hydrogen production via the ZnO/Zn water-splitting thermochemical cycle***, *16th International Symposium on the Reactivity of Solids*, Minnesota, USA, June 6, 2007.

Other Talks

L.O. Schunk: ***Solar chemical reactor engineering for the solar thermal production of zinc***, *1st SOLLAB Doctoral Colloquium on Concentrating Solar Technologies*, Cologne, Germany, October 17-18, 2005.

L.O. Schunk: ***Solar Thermal Dissociation of Zinc Oxide in a Directly-Irradiated Rotary Reactor***, *2nd SOLLAB Doctoral Colloquium on Concentrating Solar Technologies,* Monte Verità, Switzerland, October 16-18, 2006.

L.O. Schunk: ***A rotary receiver-reactor for the solar thermal dissociation of zinc oxide***, 3rd SOLLAB Doctoral Colloquium, Odeillo, France, September 11-13, 2007.

Poster

L.O. Schunk, R. Müller, P. Häberling, D. Wuillemin, A. Meier, R. Palumbo, A. Steinfeld: ***Solar Thermal Dissociation of Zinc Oxide***, *LATSIS Symposium 2006, Research Frontiers in Energy*, ETH Zürich, Switzerland, October 11-13, 2006.

Award

L.O. Schunk, P. Häberling, S. Wepf, D. Wuillemin, A. Meier, A. Steinfeld: ***A rotary receiver-reactor for the solar thermal dissociation of zinc oxide***, Best Paper Award, *ASME Energy Sustainability Conference 2007*, Long Beach, California, USA, June 27-30, 2007.

Referenzen – References

[1] R. Palumbo, A. Steinfeld, A. Meier: ***Solar Thermal Production of Zinc – Final Steps Toward Scale-Up***, *BFE*-Projekt Nr. 101050/151210, 2005-2007. Project Proposal, 2004.

[2] A. Meier: ***Solar Chemical Reactor Engineering for the Solar Thermal Production of Zinc***, *BFE*-Projekt Nr. 100323/150400, 2003-2004, Final report, May 2005.

[3] A. Steinfeld, R. Palumbo: ***Solar Thermochemical Process Technology***, In: *Encyclopedia of Physical Science and Technology*, R. A. Meyers Ed., Academic Press, Vol. 15, pp. 237-256, 2001.

[4] A. Steinfeld, A. Meier: ***Solar Fuels and Materials***, In: *Encyclopedia of Energy*, C. J. Cleveland Ed., Elsevier, Vol. 5, pp. 623-637, 2004.

[5] A. Steinfeld: ***Solar Thermochemical Production of Hydrogen - A Review***, *Solar Energy* 78, pp. 603-615, 2005.

[6] S. Abanades, P. Charvin, G. Flamant, P. Neveu: ***Screening of water-splitting thermochemical cycles potentially attractive for hydrogen production by concentrated solar energy***, *Energy* 31, pp. 2805-2822, 2006.

[7] A. Steinfeld: ***Solar hydrogen production via a two-step water-splitting thermochemical cycle based on Zn/ZnO redox reactions***, *Int. J. Hydrogen Energy* 27, pp. 611-619, 2002.

[8] C. Perkins, A.W. Weimer: ***Likely near-term solar-thermal water splitting technologies***, *Int. J. Hydrogen Energy* 29(15), pp. 1587-1599, 2004.

[9] A. Steinfeld, I. Spiewak: ***Economic evaluation of the solar thermal co-production of zinc and synthesis gas***, *Energy Conversion Management* 39, pp. 1513-1518, 1998.

[10] K. Wegner, H. Ly, R. Weiss, S. Pratsinis, A. Steinfeld: ***In-situ formation and hydrolysis of Zn nanoparticles for H_2 production by the 2-step ZnO/Zn water-splitting thermochemical cycle***, *Int. J. Hydrogen Energy* 31, pp. 55-61, 2006.

[11] F. Ernst, A. Tricoli, A. Steinfeld, S.E. Pratsinis: ***Co-Synthesis of H_2 and ZnO by in-situ Zn Aerosol Formation and Hydrolysis***, *AIChE J.* 52, pp. 3297-3303, 2006.

[12] P. Haueter, S. Möller, R. Palumbo, A. Steinfeld: ***The production of zinc by thermal dissociation of zinc oxide – solar chemical reactor design***, *Solar Energy* 67, pp. 161-167, 1999.

[13] M. Sturzenegger, I. Alxneit, H.R. Tschudi: ***Solarchemische Beiträge zur Reduktion des CO_2-Ausstosses***. *BFE*-Projekt Nr. 43708/151015, 2004-2007. Project Proposal, 2004.

[14] I. Alxneit, D. Gstöhl, C. Wieckert: ***Solarchemische Beiträge zur Reduktion des CO_2-Ausstosses***. *BFE*-Projekt Nr. 43708/151015, 2004-2007. Schlussbericht, April 2008.

[15] A. Yogev, A. Kribus, M. Epstein, A. Kogan: ***Solar "tower reflector" systems: A new approach for high-temperature solar plants***, *Int. J. Hydrogen Energy* 23, pp. 239-245, 1998.

[16] R. Osuna, R. Olavarría, R. Morillo et al.: ***PS10: Construction of a 11 MW Solar Thermal Tower Plant in Seville, Spain***, *Proc. 13th International Symposium on Concentrating Solar Power and Chemical Energy Technologies*, Seville, Spain, June 20-23, 2006. *[CD-ROM]* ISBN: 84-7834-519-1.

[17] Solúcar (Coordinator): ***10 MW Solar Thermal Power Plant for Southern Spain***, Final Technical Progress Report 2006. *EU* Project No. NNE5-1999-356, 2001-2005.

[18] W.T. Welford, R. Winston: ***High Collection Nonimaging Optics***, Academic Press, San Diego, USA, 1989.

[19] P. Haueter. T. Seitz, A. Steinfeld: ***A New High-Flux Solar Furnace for High-Temperature Thermochemical Research***, *J. Sol. Energy Eng.* 121, pp. 77–80, 1999.

[20] J. Petrasch, P. Coray, A. Meier, M. Brack, P. Haeberling, D. Wuillemin, A. Steinfeld: ***A Novel 50 kW 11,000 suns High-Flux Solar Simulator Based on an Array of Xenon Arc Lamps***, *J. Sol. Energy Eng.* 129, pp. 405-411, 2007.

[21] U. Herrmann, D.W. Kearney: ***Survey of Thermal Energy Storage for Parabolic Trough Power Plants***, *J. Sol. Energy Eng.* 124, pp. 145-152, 2002.

[22] ECOSTAR: ***European Concentrated Solar Thermal Road-Mapping***, EU-Project SES6-CT-2003-502578, Eds. R. Pitz-Paal, J. Dersch, B. Milow, DLR, 2004. http://www.vgb.org/fue_projekt252.html

[23] D. Laing, W.D. Steinmann, R. Tamme, C. Richter: ***Solid media thermal storage for parabolic trough power plants***, *Solar Energy* 80 (10), pp. 1283-1289, 2006.

[24] S. Abanades, G. Flamant: ***Solar hydrogen production from the thermal splitting of methane in a high-temperature solar chemical reactor***, *Solar Energy* 80(10), pp. 1321-1332, 2006.

[25] S. Abanades, G. Flamant: ***Production of hydrogen by thermal methane splitting in a nozzle-type laboratory scale solar reactor***, *Int. J. Hydrogen Energy* 30(8), pp. 843-853, 2005.

[26] D. Hirsch, A. Steinfeld: ***Solar Hydrogen Production by Thermal Decomposition of Natural Gas Using a Vortex-Flow Reactor***, *Int. J. Hydrogen Energy* 29, pp. 47-55, 2004.

[27] D. Trommer, D. Hirsch, A. Steinfeld: ***Kinetic Investigation of the Thermal Decomposition of CH4 by Direct Irradiation of a Vortex-Flow Laden with Carbon Particles***, *Int. J. Hydrogen Energy* 29, pp. 627-633, 2004.

[28] J.K. Dahl, K.J. Buechler, A.W. Weimer, A. Lewandowski, C. Bingham: ***Solar-thermal dissociation of methane in a fluid-wall aerosol flow reactor***, *Int. J. Hydrogen Energy* 29, pp. 725-736, 2004.

[29] S. Möller, D. Kaucic, C. Sattler: ***Hydrogen Production by Solar Reforming of Natural Gas: A Comparison Study of Two Possible Process Configurations***, *J. Sol. Energy Eng.* 128(1), pp. 16-23, 2006.

[30] A. Berman, R.K. Karn, M. Epstein: ***Kinetics of steam reforming of methane on Ru/Al2O3 catalyst promoted with Mn oxides***, *Applied Catalysis A: General* 282(1-2), pp. 73-83, 2005.

[31] A. Berman, R.K. Karn, M. Epstein: ***A New Catalyst System for High-Temperature Solar Reforming of Methane***, *Energy & Fuels* 20(2), pp. 455-462, 2006.

[32] D. Trommer, F. Noembrini, M. Fasciana, D. Rodriguez, A. Morales, M. Romero, A. Steinfeld: ***Hydrogen production by steam-gasification of petroleum coke using concentrated solar power – I. Thermodynamic and kinetic analyses***, *Int. J. Hydrogen Energy* 30, pp. 605-618, 2005.

[33] A. Z'Graggen, P. Haueter, D. Trommer, M. Romero, J.C. de Jesus, A. Steinfeld: ***Hydrogen production by steam-gasification of petroleum coke using concentrated solar power – II. Reactor design, testing, and modeling***", *Int. J. Hydrogen Energy* 31, pp. 797-811, 2006.

[34] A. Z'Graggen, P. Haueter, G. Maag, A. Vidal, M. Romero, A. Steinfeld: ***Hydrogen production by steam-gasification of petroleum coke using concentrated solar power − III. Reactor experimentation with slurry feeding***, *Int. J. Hydrogen Energy* 32, pp. 992-996, 2007.

[35] C. Wieckert et al.: ***SOLZINC: Solar carbothermic production of Zn from ZnO***, EU-Projekt Nr. ENK6-2001-00512, BBW Nr. 01.0045-1, 2001-2005.

[36] C. Wieckert, U. Frommherz, S. Kräupl, E. Guillot, G. Olalde, M. Epstein, S. Santén, T. Osinga, A. Steinfeld: ***A 300 kW solar chemical pilot plant for the carbothermic production of zinc***, *J. Sol. Energy Eng.* 129(2), pp. 190-196, 2007.

[37] E.A. Fletcher, R.L. Moen: ***Hydrogen and Oxygen from Water***, *Science* 197, pp. 1050-1056, 1977.

[38] A. Kogan: ***Direct solar thermal splitting of water and on-site separation of the products—II. Experimental feasibility study***, *Int. J. Hydrogen Energy* 23, pp. 89-98, 1998.

[39] S. Ihara: ***On the study of hydrogen production from water using solar thermal energy***. *Int. J. Hydrogen Energy* 5, pp. 527-34, 1980.

[40] E.A. Fletcher: ***Solarthermal and solar quasi-electrolytic processing and separations: zinc from zinc oxide as an example***, *Ind. Eng. Chem. Res*. 38, pp. 2275-2282, 1999.

[41] A. Steinfeld, P. Kuhn, A. Reller, R. Palumbo, J. Murray, Y. Tamaura: ***Solar-processed metals as clean energy carriers and water splitters***, *Int. J. Hydrogen Energy* 23, pp. 767-774, 1998.

[42] IPHE: ***Solar driven high temperature thermochemical production of hydrogen***, IPHE recognized project in 2005. www.iphe.net

[43] INNOHYP-CA: ***Innovative High Temperature Routes for Hydrogen Production***. *EU*-project SES6-CT-2004-513550, Completion of Roadmap, Preliminary Report USFD/DLR/CEA/06-0x, November 7, 2006. www.innohyp.com

[44] E.A. Fletcher; ***Solarthermal processing: a review***, *J. Sol. Energy Eng.* 123, pp. 63-74, 2001.

[45] R. Palumbo, J. Lédé, O. Boutin, E. Elorza Ricart, A. Steinfeld, S. Moeller, A. Weidenkaff, E.A. Fletcher, J. Bielicki: ***The production of Zn from ZnO in a high-temperature solar decomposition quench process – I. The scientific framework for the process***, *Chem. Eng. Sci.* 53, pp. 2503-2518, 1998.

[46] A. Weidenkaff, A. Reller, F. Sibieude, A. Wokaun, A. Steinfeld: ***Experimental investigations on the crystallization of zinc by direct irradiation of zinc oxide in a solar furnace***, *Chemistry of Materials* 12, pp. 2175-2181, 2000.

[47] J. Lédé, O. Boutin, E. Elorza-Ricart, M. Ferrer: ***Solar thermal splitting of zinc oxide: a review of some of the rate controlling factors***, *J. Solar Energy Eng.* 123, pp. 91-97, 2001.

[48] S. Moeller, R. Palumbo: ***The development of a solar chemical reactor for the direct thermal dissociation of zinc oxide***. *J. Solar Energy Eng.* 123, pp. 83-90, 2001.

[49] R. Müller, P. Häberling, R.D. Palumbo: ***Further Advances Toward the Development of a Direct Heating Solar Thermal Chemical Reactor for the Thermal Dissociation of ZnO(s)***, *Solar Energy* 80 (5), pp. 500-511, 2006.

[50] R. Felder: ***Well-to-wheel analysis of renewable transport fuels: Synthetic natural gas from wood gasification and hydrogen from concentrated solar energy***, Ph.D. Thesis, No. 17437, ETH Zürich, 2007.

[51] R. Felder, A. Meier: ***Well-to-Wheel Analysis of Solar Hydrogen Production and Utilization for Passenger Car Transportation***, *J. Sol. Energy Eng.* 130 (1), 011017, 2008.

[52] R. Felder, A. Meier, A. Wokaun: ***Solar Hydrogen as Future Transportation Fuel – Well-to-wheel Analysis and Economic Assessment***, *Proc. 14th International Biennial SolarPACES Concentrating Solar Power Symposium*, Las Vegas, Nevada, USA, March 4-7, 2008.

[53] R. Müller: ***Reaktor-Entwicklung für die solar thermische Produktion von Zink***, Ph.D. Thesis, Nr. 16329, ETH Zürich, 2005.

[54] L.O. Schunk, P. Haeberling, S. Wepf, D. Wuillemin, A. Meier, A. Steinfeld: ***A Receiver-Reactor for the Solar Thermal Dissociation of Zinc Oxide***, *J. Solar Energy Eng*. 130 (2), 021009, 2008.

[55] L.O. Schunk, D. Gstoehl, A. Meier, A. Steinfeld: ***Technological advances toward scale-up of solar chemical reactor for thermal ZnO decomposition***, *Proc. 14th Int. Biennial SolarPACES Concentrating Solar Power Symposium*, Las Vegas, Nevada, USA, March 4-7, 2008.

[56] D. Gstöhl, A. Brambilla, L. Schunk, A. Steinfeld: ***A Quenching Apparatus for the Gaseous Products of the Solar Thermal Dissociation of ZnO***, *Journal of Material Sciences*, in press.

[57] T. Olorunyolemi et al.: ***Thermal conductivity of zinc oxide: From green to sintered state***, Journal of American Ceramic Society 85(5), pp. 1249-1253, 2002.

[58] M.A. Clevinger, K.M. Hill, C.L. Cedeno: ***Phase Equilibria Diagrams: Phase diagrams for ceramists***, *1995 cumulative indexes : volumes 1-11, Annuals '91-'93, High Tc monograph*, Westerville, Ohio: The American Ceramic Society, 1995.

[59] V. Gianini: ***Solar Thermogravimetric Material Tests for a Solar Reactor***, Bachelor Thesis, ETH Zürich, 2006.

[60] L.O. Schunk, A. Steinfeld: ***Thermal dissociation kinetics of ZnO exposed to concentrated solar irradiation using a solar-driven thermogravimeter in the range 1800-2100 K***, AIChE Journal, submitted January 2008.

[61] S. Möller, R. D. Palumbo: ***Solar thermal decomposition kinetics of ZnO in the temperature range 1950-2400K***, *Chemical Engineering Science* 56(15), pp. 4505-4515, 2001.

[62] D. Kronenberg: ***Experimental investigation of the solar thermal dissociation of ZnO in a rotary reactor***, Semester Thesis, PSI Villigen and ETH Zürich, March 2007.

[63] E. Guglielmini: ***ZnO/Zn Thermochemical Cycle: CFD Modeling of the Quench Unit for Zn/O2 Separation***, Semester Thesis, PSI Villigen and ETH Zürich, July 2007.

[64] C. Suter: ***Development and experimental investigation of a quench unit for a solar thermal rotary reactor***, Master Thesis, PSI Villigen and ETH Zürich, April 2008.

[65] I. Alxneit: ***Quenching a Stoichiometric Mixture of Zinc Vapor and Oxygen – Model Calculations***, *Solar Energy*, in press.

[66] S. Meder: ***Modification of test reactor SOLAR-TG and accomplishment of material tests***, Bachelor Thesis, ETH Zürich, 2005.

[67] L.O. Schunk: ***Solar Thermal Dissociation of Zinc Oxide: High-Temperature Receiver-Reactor Modeling and Experimentation***, ETH Zürich, Switzerland, to be submitted 2008.

[68] A.K. Galwey, M.E. Brown: ***Thermal Decomposition of Ionic Solids***, Amsterdam: Elsevier, 1999.

[69] B.V. L'Vov: ***Recent advances in absolute analysis by graphite furnace atomic absorption spectrometry***, *Spectrochimica Acta Part B: Atomic Spectroscopy* 45(7), pp. 633-655, 1990.

[70] L.O. Schunk, W. Lipiński, A. Steinfeld: ***Numerical and Experimental Study on Ablation and Sintering of Zinc Oxide under Direct High-Flux Irradiation***, *AIChE Journal*, to be submitted 2008.

[71] L.O. Schunk, W. Lipiński, A. Steinfeld: ***Transient numerical model of a directly irradiated receiver-reactor for the solar thermal dissociation of zinc oxide***, to be submitted 2008.

[72] F.P. Incropera, D.P. Dewitt: ***Fundamentals of Heat and Mass Transfer***, John Wiley & Sons, New York, 1996.

[73] Y.R. Shieh, C.J. Li, Y.H. Hung: **Heat transfer from a horizontal wafer-based disk of multi-chip modules**, Int. J. Heat and Mass Transfer 42(6), pp 1007-1022, 1999.

[74] R. Siegel, J. Howell: ***Thermal Radiation Heat Transfer***, Taylor & Francis, New York, London, 2002.

[75] J. Petrasch: ***Thermal Modeling of Solar Chemical Reactors: Transient Behavior, Radiative Transfer***, Diploma Thesis, ETH Zürich, 2002.

[76] P. Leu: ***Untersuchung einer Tornado-Gasführung im ZIRRUS Solarreaktor mit CFD***, Master Thesis, ETH Zürich, 2006.

[77] C. Suter: ***CFD Modeling of a Solar Reactor for the Thermal Decomposition of Zinc Oxide***, Semester Thesis, PSI Villigen and ETH Zürich, July 2007.

[78] *ANSYS CFX 10.0*, 2005: http://www.ansys.com/products/cfx.asp.

[79] A. Kogan, M. Kogan: ***The Tornado Flow Configuration - An Effective Method for Screening of a solar Reactor Window***, *J. Solar Energy Eng*. 124, pp. 206-214, 2002.

[80] K. Grunert: ***Untersuchungen zur Turbulenzmodellierung und Berechnung verdrallter Innenströmungen***, Ph.D. Thesis, Technische Universität Berlin, Germany, 2000.

[81] A. Meier, A. Steinfeld: ***Towards Industrial Solar Production of Zinc and Hydrogen – Reactor Optimization and Scale-Up***, BFE-Projekt Nr. 102420/153045, 2008-2011.

Anhang – Appendix

The following is a list of major publications closely related to the current *Solar Zinc Project* [1]. Included are also publications that describe work of the previous *BFE* project [2] and were published during the reporting period of the current project.

Peer-reviewed Journals

I. Alxneit, H.R. Tschudi: ***A Kinetic Model for the Formation of Incompletely Oxidized Metal Oxide Aerosols***, *J. Aerosol Sci.*, submitted 2008.

I. Alxneit: ***Quenching a Stoichiometric Mixture of Zinc Vapor and Oxygen – Model Calculations***, *Solar Energy*, in press.

D. Gstöhl, A. Brambilla, L. Schunk, A. Steinfeld: ***A Quenching Apparatus for the Gaseous Products of the Solar Thermal Dissociation of ZnO***, *Journal of Material Sciences*, in press.

T. Melchior, C. Perkins, A.W. Weimer, A. Steinfeld: ***A Cavity-Receiver Containing a Tubular Absorber for High-Temperature Thermochemical Processing using Concentrated Solar Energy***, *International Journal of Thermal Sciences*, in press.

T. Melchior, A. Steinfeld: ***Radiative transfer within a cylindrical cavity with diffusely/specularly reflecting inner walls containing an array of tubular absorbers***, *J. Sol. Energy Eng.*, in press.

M. Epstein, G. Olalde, S. Santén, A. Steinfeld, C. Wieckert: ***Towards an industrial solar carbothermic production of zinc***, *J. Sol. Energy Eng.* 130 (1), 014505, 2008.

R. Felder, A. Meier: ***Well-to-Wheel Analysis of Solar Hydrogen Production and Utilization for Passenger Car Transportation***, *J. Sol. Energy Eng.* 130 (1), 011017, 2008.

R. Müller, W. Lipinski, A. Steinfeld: ***Transient heat transfer in a directly-irradiated solar chemical reactor for the thermal dissociation of ZnO***, *Applied Thermal Engineering* 28 (5-6), pp. 524-531, 2008.

R. Müller, A. Steinfeld: ***H_2O-splitting thermochemical cycle based on ZnO/Zn-redox: Quenching the effluents from the ZnO dissociation***, *Chemical Engineering Science* 63 (1), pp. 217-227, 2008.

L.A. Dombrovsky, W. Lipinski, A. Steinfeld: ***A diffusion-based approximate model for radiation heat transfer in a solar thermochemical reactor***, *Journal of Quantitative Spectroscopy and Radiative Transfer* 103, pp. 601-610, 2007.

M. Karlsson, I. Alxneit, F. Rütten, D. Wuillemin, H.R. Tschudi: ***A Compact Setup to Study Homogeneous Nucleation and Condensation***, *Rev. Sci. Instrum.* 78, 34102, 2007.

S. Kräupl, C. Wieckert: ***Economic evaluation of the solar carbothermic reduction of ZnO by using a single sensitivity analysis and a Monte-Carlo risk analysis***, *Energy* 32 (7), pp. 1134-1147, 2007.

R. Müller, A. Steinfeld: ***Band-Approximated Radiative Heat Transfer Analysis of a Solar Chemical Reactor for the Thermal Dissociation of Zinc Oxide***, *Solar Energy* 81 (10), pp. 1285-1294, 2007.

J. Petrasch, P. Coray P., A. Meier, M. Brack, P. Haeberling, D. Wuillemin, A. Steinfeld: ***A Novel 50-kW 11,000 Suns High-Flux Solar Simulator Based on an Array of Xenon Arc Lamps***, *J. Sol. Energy Eng.* 129 (4), pp. 405-411, 2007.

C. Wieckert, U. Frommherz, S. Kräupl, E. Guillot, G. Olalde, M. Epstein, S. Santén, T. Osinga, A. Steinfeld: ***A 300 kW solar chemical pilot plant for the carbothermic production of zinc***, *J. Sol. Energy Eng.* 129 (2), pp. 190-196, 2007.

F. Ernst, A. Tricoli, A. Steinfeld, S.E. Pratsinis: ***Co-Synthesis of H_2 and ZnO by in-situ Zn Aerosol Formation and Hydrolysis***, *AIChE J.* 52, pp. 3297-3303, 2006.

C. Guesdon, I. Alxneit, H.R. Tschudi, D. Wuillemin, Y. Brunner, L. Winkel and M. Sturzenegger: ***1 kW Imaging Furnace - A Tool for High-Temperature Chemical Reactivity Studies***; *Solar Energy* 80, pp. 1344ff, 2006.

C. Guesdon, I. Alxneit, H.R. Tschudi, D. Wuillemin and M. Sturzenegger: ***A 1 kW Imaging Furnace with in-situ Measurement of Surface Temperature***, *Rev. Sci. Instrum.* 77, 035102, 2006.

S. Kräupl, U. Frommherz, C. Wieckert: ***Solar Carbothermic Reduction of ZnO in a Two-Cavity Reactor: Laboratory Experiments for a Reactor Scale-Up***, *J. Sol. Energy Eng.* 128 (1), pp. 8-15, 2006.

W. Lipiński, A. Steinfeld: ***Annular Compound Parabolic Concentrator***, *J. Sol. Energy Eng.* 128 (1), pp. 121-124, 2006.

W. Lipinski, D. Thommen, A. Steinfeld: ***Unsteady radiative heat transfer within a suspension of ZnO particles undergoing thermal dissociation***, *Chemical Engineering Science* 61, pp. 7029-7035, 2006.

R. Müller, P. Häberling, R.D. Palumbo: ***Further Advances Toward the Development of a Direct Heating Solar Thermal Chemical Reactor for the Thermal Dissociation of ZnO(s)***, *Solar Energy* 80 (5), pp. 500-511, 2006.

K. Wegner, H. Ly, R. Weiss, S. Pratsinis, A. Steinfeld: ***In-situ formation and hydrolysis of Zn nanoparticles for H_2 production by the 2-step ZnO/Zn water-splitting thermochemical cycle***, *Int. J. Hydrogen Energy* 31, pp. 55-61, 2006.

J.K. Dahl, A.W. Weimer, A. Z'Graggen, A. Steinfeld: ***Two-Dimensional Axi-Symmetric Model of a Solar-Thermal Fluid-Wall Aerosol Flow Reactor***, *J. Sol. Energy Eng.* 127 (1), pp. 76-85, 2005.

A.P. Freid, P.K. Johnson, M. Musella, R. Mueller, J.E. Steinbrenner, R.D. Palumbo: ***Solar Blind Pyrometer Temperature Measurements in High Temperature Solar Thermal Reactors: A Method for Correcting the System-Sensor Cavity Reflection Error***, *J. Solar Energy Eng.* 127, pp. 86-93, 2005.

S. Kräupl, A. Steinfeld: ***Monte Carlo Radiative Transfer Modeling of a Solar Chemical Reactor for The Co-Production of Zinc and Syngas***, *J. Sol. Energy Eng.* 127 (1), pp. 102-108, 2005.

W. Lipiński, A. Z'Graggen, A. Steinfeld: ***Transient radiation heat transfer within a non-gray non-isothermal absorbing-emitting-scattering suspension of reacting particles undergoing shrinking***, *Numerical Heat Transfer Part B: Fundamentals* 47 (5), pp. 443-457, 2005.

A. Steinfeld: ***Solar Thermochemical Production of Hydrogen - A Review***, *Solar Energy* 78, pp. 603-615, 2005.

R. Weiss, H. Ly, K. Wegner, S. Pratsinis, A. Steinfeld: ***H_2 Production by Zn hydrolysis in a hot-wall aerosol reactor***, *AIChE Journal* 51, 1966-1970, 2005.

C. Wieckert: ***Design Studies for a Solar Reactor Based on a Simple Radiative Heat Exchange Model***, *J. Sol. Energy Eng.* 127 (3), pp. 425-429, 2005.

Ph.D. Theses

R. Müller: ***Reaktor-Entwicklung für die solar thermische Produktion von Zink***, Ph.D. Thesis, Nr. 16329, ETH Zürich, 2005.

M. Karlsson: ***Nucleation and condensation in a stationary supersonic flow***, Ph.D. Thesis, Nr. 16542, ETH Zürich, 2006.

P. Bodek: ***Design, Construction and Characterization of a Coaxial Nozzle to Study Reaction Kinetics***, Ph.D. Thesis, Nr. 17123, ETH Zürich, 2007.

R. Felder: ***Well-to-wheel analysis of renewable transport fuels: Synthetic natural gas from wood gasification and hydrogen from concentrated solar energy***, Ph.D. Thesis, No. 17437, ETH Zürich, 2007.

Bachelor / Diploma / Master Thesis

C. Meier: ***Kalorimeter-Messungen am PSI High-Flux Solar Simulator***, Bachelor Thesis, PSI Villigen and ETH Zürich, 2006.

C. Zimmermann: ***Untersuchung der turbulenten Grenzschicht einer Lavaldüse mittels CFD-Modellierung***, Master Thesis, PSI Villigen and ETH Zürich, 2006.

A. Brambilla, D. Colzani: ***Solar Thermochemical Process: Investigation of Zinc Separation from a $Zn_{(g)}/O_2$ Mixture***, Master Thesis, Politecnico di Milano, ETH Zürich, and PSI Villigen, March 2007.

Semester Theses

R. Hotz: ***Untersuchung des Quenchverhaltens von Zink/Sauerstoffgemischen in einem Quarzglasreaktor***, Semester Thesis, ETHZ, 2005.

M. Molotta: ***Analysis, Modification and Design of a Heat Exchanger for the REKIN Experiment***, Semester Thesis, ETHZ, 2005.

D. Siegrist: ***Konzeptionierung einer Hochtemperatur-Stickstoffheizung***, Semester Thesis, PSI Villigen and ETH Zürich, 2005.

F. Wiedmer: ***Kalorimetermessungen eines stark strahlenden Sonnensimulators***, Semester Thesis, PSI Villigen and ETH Zürich, 2005.

J.-F. Feldhoff: ***Temperature measurements in cavities by radiation pyrometry – Laser assisted single wavelength pyrometry***, Semester Thesis, PSI Villigen and ETH Zurich, 2006.

D. Wiesmann: ***FEWS Measurement of the Partial Pressure of Zinc***, Semester Thesis, PSI Villigen and ETH Zürich, 2006.

K. Cuche: ***Experimental investigation of the quench unit for $Zn_{(g)}/O_2$ separation***, Semester Thesis, PSI Villigen and ETH Zürich, July 2007.

M. Gasser, F. Lienhard: ***Energietransportoptionen – Ein Vergleich zwischen Wasserstoffpipeline und Hochspannungs-Gleichstrom-Übertragung***, Semester Thesis, PSI Villigen and ETH Zürich, March 2007.

E. Guglielmini: ***ZnO/Zn Thermochemical Cycle: CFD Modeling of the Quench Unit for Zn/O2 Separation***, Semester Thesis, PSI Villigen and ETH Zürich, July 2007.

Conference Proceedings

R. Felder, A. Meier: ***Well-To-Wheel Analysis of Solar Produced Hydrogen for Future Transportation Systems***, *Proc. 16th World Hydrogen Energy Congress (WHEC 16)*, Lyon, France, June 13-16, 2006.

R. Felder, A. Meier: ***Well-to-Wheel Analysis of Solar Hydrogen Production and Utilization for Passenger Car Transportation***, *Proc. 13th SolarPACES International Symposium*, Seville, Spain, June 20-23, 2006.

F. Rütten, I. Alxneit, H.R. Tschudi: ***Kinetics of homogeneous nucleation and condensation of n-butanol at high supersaturation***, Proc. 17th Int. Conf. on Nucleation and Atmospheric (submitted to Atmospheric Research), Galway, Ireland, August 13-17, 2007.

F. Rütten, I. Alxneit, H.R. Tschudi: ***Challenges in the thermochemical water-splitting cycle based on the ZnO/Zn redox pair: Rapid quench and nucleation of zinc***, Proc. 17th Int. Conf. on Nucleation & Atmospheric Aerosols, Galway, Ireland, August 13-17, 2007.

R. Felder, A. Meier, A. Wokaun: ***Solar Hydrogen as Future Transportation Fuel – Well-to-wheel Analysis and Economic Assessment***, *Proc. 14th Int. Biennial SolarPACES Concentrating Solar Power Symposium*, Las Vegas, Nevada, USA, March 4-7, 2008.

Articles in Magazines and Newsletters

A. Meier, A. Steinfeld: ***Für eine nachhaltige Energieversorgung***, *GWA* 3, pp. 217-223, 2005.

A. Meier, C. Wieckert, A. Steinfeld: ***Wasserstoff aus Wasser und Sonnenenergie – Hochtemperatur-Solarchemie***, Bulletin SEV/VSE 24/25, 2005, pp. 11-17.

Green Hydrogen Production, *Chemical Engineering Progress*, p. 8, March 2006.

Nachhaltige Herstellung von Wasserstoff mit konzentrierter Sonnenenergie, *Novatlantis* Nr. 6, p. 5, 2006.

Storing solar energy, *REFOCUS*, Vol. 7, No. 5, pp. 32-36, 2006.

Tu die Sonne in den Tank, *SAFT & KRAFT* – Magazin der Elektrizitätswerke des Kantons Zürich, No. 4, pp. 14-15, 2006.

Wasserstoff vom Sonnenturm, Deutschlandradio, 16.06.2006, http://www.dradio.de/dlf/sendungen/forschak/511553

A. Steinfeld: ***Mit der Kraft von 10'000 Sonnen***, NZZ Executive, May 20, 2007.

A. Steinfeld: ***Die Sonne macht Chemie***, Swiss Engineering STZ 12-13, May 2007.

A. Steinfeld: ***Die Sonne als Pulver hin- und herfahren***, SonntagsZeitung 61-62, July 15, 2007.

A. Meier: ***Task II: Solar Chemistry***, International Energy Agency – SolarPACES Annual Report 2007, M. Geyer ed., Chapter 4, 2008.

A. Meier: ***Task II: Solar Chemistry***, International Energy Agency – SolarPACES Annual Report 2006, M. Geyer ed., Chapter 4, 2007.

A. Meier: ***Task II: Solar Chemistry***, International Energy Agency – SolarPACES Annual Report 2005, M. Geyer ed., Chapter 4, 2006.

PSI Scientific Reports

A. Meier, M. Brack, P. Coray, P. Häberling, D. Wuillemin, J. Petrasch, A. Steinfeld: ***High-flux solar simulator for high-temperature thermochemical research***, *PSI Scientific Report 2005 / Volume 3*, pp. 16-17, 2006.

I. Alxneit, D. Gstöhl, F. Rütten, H. R. Tschudi, C. Wieckert, D. Wuillemin, A. Steinfeld: ***The rapid quench – a challenge for the water-splitting thermochemical ZnO/Zn cycle***, *PSI Scientific Report 2006*, pp. 74-75, 2007.

Invited Talks

A. Meier: ***PSI solar simulator for solar chemistry research,*** Inauguration of PSI's High-Flux Solar Simulator, PSI, Switzerland, November 4, 2005.

A. Steinfeld: ***Brennstoffe aus Sonnenlicht,*** Naturforschende Gesellschaft Graubünden, Chur, January 13, 2005.

A. Steinfeld: ***Solar fuels for CO_2 mitigation,*** Anorganisch-chemisches Institut, Universität Zürich, January 21, 2005.

A. Steinfeld: ***Advances in solar thermochemical process technology,*** Weizmann Institute of Science, Israel, April 4, 2005.

A. Steinfeld: ***Present status and future prospects of the production of hydrogen using concentrating solar technologies,*** DOE Solar Energy Workshop, April 18, 2005.

A. Steinfeld: ***Thermochemical processing of hydrogen from water,*** Florida Solar Energy Center, USA, July 7, 2005.

A. Steinfeld: ***Co-synthesis of H2 and ZnO nanoparticles by in-situ Zn aerosol formation and hydrolysis,*** University of Colorado, Boulder, July 8, 2005.

A. Steinfeld: ***Tutorial – thermochemical and electrochemical production of hydrogen,*** ASME Int. Solar Energy Conference, Orlando, August 9, 2005.

A. Steinfeld: ***Die Forschung im Bereich Erneuerbare Energien,*** Weiterbildungsseminar des Forum VERA, Meiringen, September 23, 2005.

A. Steinfeld: ***Overview of solar hydrogen production – the barriers, the needs, and the challenges,*** IPHE Renewable Hydrogen Workshop, Seville, October 25, 2005.

C. Wieckert: ***Zinc stores solar energy: Pilot scale carbothermic reduction of ZnO using concentrated solar light,*** 53rd Zinc Experts Committee Meeting of the GDMB (Society for Mining, Metallurgy, Resource and Environmental Technology), Luxembourg, December 7-9, 2005.

A. Meier: ***Hochtemperatur-Solarchemie – Sonnenenergie konzentrieren und chemisch speichern,*** *LOG-Kolloquium*, PSI, Villigen, August 31, 2006.

A. Steinfeld: ***Solar Thermochemical Process Technology***, UOP/Honeywell Invitational Lecture Series, Chicago, March 21, 2006.

A. Steinfeld: ***Solar Thermochemical Production of Hydrogen,*** University of Illinois, Chicago, March 20, 2006.

A. Steinfeld: ***A closer look at the potential of renewable energy sources,*** VERA Forum, Böttstein, September 18, 2006.

A. Steinfeld: ***Renewable Energy***, Academia Engelberg, Engelberg, October 9, 2006.

A. Steinfeld: ***Thermochemical reactor technology for solar fuels production,*** LATSIS Symposium, ETH Zurich, October 13, 2006.

I. Alxneit: ***Aerosol Synthesis Including Chemical Reaction(s)***, University of Milano, Italy 2007.

P. Coray, J. Petrasch, A. Meier, P. Häberling, D. Wuillemin, S. Wepf, A. Steinfeld: ***The PSI's High-Flux Solar Simulator for high-temperature thermochemical research***, 10. Kölner Sonnenkolloquium, DLR, Köln-Porz, Germany, June 21, 2007.

A. Meier, A. Steinfeld: ***A close look at the potential of renewable energy sources***, Swiss Physical Society Annual Meeting, University of Zürich Irchel, February 20, 2007.

A. Meier, A. Steinfeld: ***The ultimate goal: Solar hydrogen production***, World Solar Power 2007, Seville, Spain, October 26, 2007.

A. Steinfeld: ***Solar energy and energy efficiency,*** EU's Joint Research Centres Information Event, Eawag Dübendorf, March 16, 2007.

A. Steinfeld: ***Advances in the solar thermochemical production of fuels,*** Mechanical Engineering Founders Lecture of the University of Minnesota, Minneapolis, USA, April 11, 2007.

A. Steinfeld: ***Concentrated solar energy: power, storage, and fuels,*** ALSTOM, Birr, September 20, 2007.

A. Steinfeld: ***Solar thermochemical production of hydrogen – present status and future prospects,*** Clavin W. Rice Award Lecture, ASME Congress, Seattle, USA, November 13, 2007.

A. Steinfeld: ***Solar thermal power and fuels,*** Bat-Sheva Seminar, Haifa, Israel, September 2, 2007.

Other Talks

A. Steinfeld: ***Wasserstoff aus Wasser und Solarenergie****,* 150 ETH-Professorinnen und Professoren im Gespräch, Zürich, April 23, 2005.

A. Steinfeld: ***Chemical energy carriers from the sun****,* ETSF-5 Energy Technologies for a Sustainable Future, PSI, June 10, 2005.

C. Wieckert: ***Carbothermic solar ZnO reduction for solar hydrogen production****,* SOLLAB Solar Colloquium: "Solar Hydrogen", Cologne/Germany, June 14, 2005.

P. Coray: ***Performance characterisation of PSI's high flux solar simulator***, *2nd SOLLAB Doctoral Colloquium on Concentrating Solar Technologies,* Monte Verità, Switzerland, October 16-18, 2006.

R. Felder: ***Well-to-wheel analysis of the production of solar hydrogen and its use in future passenger cars***, *2nd SOLLAB Doctoral Colloquium on Concentrating Solar Technologies,* Monte Verità, Switzerland, October 16-18, 2006.

F. Rütten: ***Design and modeling of an experiment based on a Laval nozzle to study homogeneous nucleation***, *2nd SOLLAB Doctoral Colloquium on Concentrating Solar Technologies,* Monte Verità, Switzerland, October 16-18, 2006.

A. Steinfeld: ***Research Highlights at the Professorship of Renewable Energy Carriers****,* 6th Forum Thermo- and Fluid Dynamics, ETH Zurich, November 24, 2006.

P. Coray: ***Experimental determination of radiative properties for modelling radiation heat transfer in semi-transparent materials***, 3rd SOLLAB Doctoral Colloquium, Odeillo, France, September 11-13, 2007.

R. Felder, A. Meier: ***Well-to-wheel analysis of solar produced hydrogen for future passenger car transport systems***, 3rd International Conference on Life Cycle Management, LCM 2007, Zurich, Switzerland, August 27-29, 2007.

A. Meier, R. Felder: ***Life Cycle Assessment of Hydrogen Production Using Concentrating Solar Power Technologies***, Swiss Physical Society Annual Meeting, University of Zürich Irchel, February 20, 2007.

F. Rütten: ***Homogeneous nucleation of zinc vapour***, 3rd SOLLAB Doctoral Colloquium, Odeillo, France, September 11-13, 2007.

Posters

I. Alxneit, H.R. Tschudi: ***Modelling the formation of metal oxide aerosols***, European Aerosol Conference, University of Salzburg, Austria, September 9-14, 2007.

C. Wieckert: ***SOLZINC - Solar carbothermic production of Zn from ZnO***, EU Hydrogen and Fuel Cell Technical Review Days, Brussels, Belgium, October 10-11, 2007.

Award

A. Meier, C. Wieckert, A. Steinfeld: ***Wasserstoff aus Wasser und Sonnenenergie – Hochtemperatur-Solarchemie***, *Bulletin SEV/VSE* **24/25**, 11-17, 2005. Awarded the "Electrosuisse Fachliteraturpreis 2006".